

Full length article

In-situ observation and calibration for structure safety diagnosis through finite element analysis and mixed reality

Xuefeng Zhao, Wangbing Li, Zhe Sun^{*}, Meng Zhang, Lingli Huang

Faculty of Architecture, Civil and Transportation Engineering, Beijing University of Technology, Beijing 100124, China



ARTICLE INFO

Keywords:

Structure safety diagnosis
Mixed reality
Finite element analysis
In-situ

ABSTRACT

In-situ observation and calibration through non-intrusive approaches are necessary for diagnosing structural safety risks and predicting structure deterioration patterns during field inspections of critical civil infrastructures. Conventional visual inspections always subject to engineering knowledge and field experiences, which could hardly examine structure risks under as-is conditions. Finite Element Analysis (FEA) tools and model updating algorithms could help examine changes of stress and displacements under extreme environmental conditions according to the discovered structure defects and spatiotemporal changes. However, such tools usually require extensive computing resources for running simulations at a location that is usually far from the jobsite. Mixed Reality (MR) techniques could help in visualizing the virtual geometric composition of physical structural components. Unfortunately, existing MR device could hardly visualize tedious FEA and model updating processes of critical structural components. Integrated used of FEA tools and MR techniques could help support real-time safety diagnosis of critical structural components at remote locations. In this study, the authors established a framework that integrate sensing techniques, FEA tools, model updating algorithms, and MR for supporting structure safety diagnosis of civil infrastructures. The proposed method aims to 1) capture and analyze structural defects, 2) calibrate the virtual model with the real structure for visualizing FEA results of critical structural components through MR. The authors validate the proposed method through a case study. Results show that the proposed method provides fundamental support for effective on-site structure safety diagnosis.

1. Introduction

Traditional visual inspections for examining structure conditions are time consuming and may subject to engineers' experiences. How to achieve effective and precise structure condition assessments is vital to ensure structure safety. Finite element analysis (FEA) is a widely used numerical simulation method in various engineering domains (e.g., in civil engineering) [1–3]. Structure defects captured onsite could be used for updating the FE model and examine structure conditions under various scenarios. Existing FEA tools are powerful in analyzing structural dynamics through simulations. Unfortunately, the entire structure analysis processes (pre-processing, solving, post-processing) still requires engineers to operate on a computer remotely from the actual jobsite [4]. Challenges still exist for examining structural conditions through FEA simulations and visualizing stress distributions of structure components at remote locations. For instance, (1) traditional FEA can only be performed in a purely virtual environment, which isolates the

human perception of real space (e.g., scale and direction); (2) traditional FEA processes used for the preview (i.e., structural design [5]) or inversion (i.e., structural health monitoring [6]) of the real structural components are usually detached from the real structural components, creating challenges in performing real-time FEA based on the state data of the real structural components. It is thus necessary to establish a method that automates the condition assessment process and allows structure engineers to conduct field visual inspection and examine structure conditions in real-time.

As immersive technologies, augmented reality (AR) / virtual reality (VR) / mixed reality (MR) have become one of the significant digital intelligence forms in the digital transformation of complex systems [7,8]. Integrating AR/VR/MR technologies with digital transformation can empower businesses and facilitate value creation [9–11]. As an emerging immersive technology, MR combines the physical and virtual worlds to create a new mixed-reality space that allows multidimensional interactions among human, computers, and environments [12]. Such

^{*} Corresponding author.

E-mail addresses: zhaoxuefeng@bjut.edu.cn (X. Zhao), liwangbing@emails.bjut.edu.cn (W. Li), zhesun@bjut.edu.cn (Z. Sun), zm@emails.bjut.edu.cn (M. Zhang), huangll123@emails.bjut.edu.cn (L. Huang).

<https://doi.org/10.1016/j.aei.2024.102415>

Received 4 May 2023; Received in revised form 31 January 2024; Accepted 12 February 2024

Available online 21 February 2024

1474-0346/© 2024 Elsevier Ltd. All rights reserved.

enhanced interactions allow engineers to augment their understanding of the physical environment with digital information. MR technology has been widely adopted in manufacturing [13], construction [14,15], the medical industry [16], education [17,18], and many other domains. However, MR devices (e.g., HoloLens 2) are only used to present a virtual geometric composition of the physical world in the use cases mentioned above. The implementation of MR rarely includes the intrinsic mechanisms and conditions of the physical world (e.g., stress and deformation of the structural components). Moreover, very limited studies and development exist for fully use of the computing power of MR devices.

This study proposed a method that integrates the FEA and MR to solve the two main challenges in combining the human perception of real physical space and performing real-time FEA based on the state data of the real structural components in FEA utilization. Based on the attribute set parameters of real structural components and the mechanism presentation form of spatial gridding chromaticity filling, the authors innovatively define the mechanical mechanism of real structural components in the virtual world by creating virtual structural components. Besides, the authors have achieved the development and application of the real-time FEA calculation of real structural components based on the computing power of MR devices. The results obtained show that real-time FEA calculations can be performed in the MR device using the state data of real structural components. Taking advantage of the integration of the real world and virtual world in MR, this study uses the in-situ coordinates of real structural components as the spatial anchor point of MR and superimposes the FEA results generated by the real-time calculation in the MR device with the real structural components to realize the interactive real-time FEA of structural components in situ. It is worth mentioning that the research in this paper is mainly based on MR devices combined with state parameters of critical structural components in engineering sites for interactive finite element analysis. Similar investigations are still uncommon, and this paper only covers the core and basic methodology framework, which is presently undergoing validation and testing in laboratories. For practical engineering applications, the method proposed in this paper still needs many additions and improvements, so this part will not be discussed.

The main contributions of this study include: (1) establishing a MR-enabled standalone real-time finite element analysis system that avoids external computing and processing equipment and data transfer processes and provides fundamental support for effective field structure safety diagnosis, (2) calibration and augmented visualization of finite element data in the virtual-physical fusion environment for intuitive observation and agile structural safety diagnosis, (3) the implicit and invisible internal force status of the structure is calculated in situ and explicitly visualized, achieving visual perspective and enhancing human's perception of the engineering system.

2. Literature review

2.1. FEA applications for infrastructure structure

Finite Element Analysis (FEA) is best suitable method for modeling and analysis of complex problem with all physical situations (Dhades et al. [19]), like optimized design of new engineering components (Erdal et al. [20]), preview of the phases of construction (Hoffman et al. [21]) and et al. However, due to a large number of degrees of freedom (DoF) and complex interactions between elements, finite element analysis has high computational costs (Dang et al. [22]). Therefore, FEA applications for infrastructure structures usually rely on FEA software (e.g., SAP2000 (Gharad et al. [23], Diz-Mellado et al. [24]), Abaqus, etc.) in computers with sufficient computing power (e.g., laptops, workstations, etc.) remotely which reduces the flexibility of the FEA application site. Recent studies have also employed AI-driven approaches like neural networks to predict internal forces [25]. Digital twins (DT) are vital and emerging directions in the field of infrastructure structure and its digital

transformation (Jiang et al. [26] and Su et al. [27]). Real-time FEA is essential and plays a key role as a supporting technology for DT (Rios et al. [28]). Real-time state data from the physical world is transmitted to validate, update and compute the FE model, enabling real-time condition assessment (Moi et al. [29]) and reliability prediction (Wang et al. [30]). In the implementation of real-time FEA, data transfer processes are indispensable. Moreover, current FEA tools rely on desktop virtual environment (VE), but this purely VE often cannot accurately represent physical structures and access actual physical context, leading to a lack of intuitiveness and efficiency in examining FE models and interpreting FEA results (Ong and Huang [31]). This also creates an unintuitive human perception of engineered systems.

At present, FEA has been utilized in many aspects of civil engineering domain. The execution of FEA requires significant computational costs, which is usually supported by external computing and processing equipment. Therefore, the data transfer process is necessary when performing real-time FEA using real-time physical state data. The high computational costs and the necessary data transfer processes pose challenges to the implementation of real-time FEA. In addition, VE-dependent FEA visualizations isolate the physical context and make it difficult to intuitively perceive the engineered system.

2.2. Augmented visualization for FEA

To take the FEA visualization away from VE and make it more intuitive and interactive, some studies have examined the augmented display for FEA. Augmented reality (AR) is an important digital simulation and visualization technology that can improve the efficiency of manufacturing system operations and digitalization (Dimitris Mourtzis [32,33]). Olbrich et al. [34] implemented the traditional finite element method on a simulation server with AR devices and delivered snapshots to AR applications for real-time visualization. The FEA computational part of this study is still performed on bulky servers. AR is only used as a planar visualization tool, changing only the post-processing aspect of traditional FEA. Seo et al. [35] proposed a method that integrates the FEA method with an AR-based mechanical product simulation platform to achieve the effective design of an engineering product. In this paper, FEA results was calculated through web-based FEA service and AR was only used as a visualization tool. Mourtzis et al. [36–38] proposed an Industrial Internet of Things (IIoT) framework for the simulation and visualization of selected monitored values based on AR/MR and CFD in a cloud-computing environment for the intuitive visualization of the data, in which ANSYS Fluent simulation software is used as a calculation module on a PC application. And the data analysis and visualization application Paraview served as middleware from the simulation results to the MR environment. The above literature demonstrates the great contribution of augmented visualization of FEA to the perception of manufacturing and engineering systems. However, with the evidence so far, the computational module of FEA is usually performed in external devices and AR/MR is only used as a visualization tool for FEA data. In other words, the computational and visualization modules of FEA are separated at the current stage.

Moreover, AR can not only take the FEA visualization away from VE, but also superimpose the FEA results onto physical objects. Yavuz Erkek et al. [39] performed a modal analysis of an aluminum impeller using the finite element method and superimposed the digital information on the real aluminum impeller model via augmented reality with Unity Vuforia Model Target. AR rigidly superimposes virtual images on real objects in this study and provides a new means for designers and engineers to visualize modal analysis results. But the sense of interactive experience brought to designers and engineers is inadequate. Muthalif et al. [40] proposed a classification of AR visualization methods and conducted a comparative analysis of existing methods, emphasizing the importance of improving depth perception and positional accuracy. Huang et al. [41] presented a system which integrates sensor measurement and real-time FEA simulation into an AR-based environment for

the purpose of enhancing structural analysis with augmented reality technologies. In this paper, QR codes printed on paper were used as registration points for AR virtual images. The above case virtual-physical calibration is done by registering the virtual content to the physical object through marker-based image recognition. In this way, the position of the virtual content in the physical world is bound to the marker. As a result, it is more like a virtual presentation technology. However, for complex outdoor construction sites, marker-based registration points can be easily damaged and it is full of challenges to arrange markers on large civil engineering structures. Therefore, at this stage the virtual-physical calibration approach is usually only realized on small scale scenarios. Virtual-physical calibration and in-situ visualization are still limited and challenging in large-scale scenarios, especially in civil engineering infrastructure structures.

Further, interaction is another important part of augmented visualization for FEA. Turkan et al. [42] introduced a new pedagogy for teaching structural analysis that incorporates mobile AR through iPad and interactive 3D visualization technology. This study enhanced the contents of structural analysis textbooks by visualizing discrete structural members to illustrate how structures behave under different loading conditions. In this study, the user achieved control of the virtual content by changing parameters on the screen of the AR vehicle (i.e., iPad). In other words, the interaction was realized through the screen rather than a direct manipulation of the virtual content. Omg and Huang et al. [4,31,43,44] proposed a novel system which integrates sensor measurement, FEA simulation (running in Ansys), and scientific visualization into an AR-based environment. In this system, input data could be acquired using sensors and FEA results could be visualized directly on physical objects. Visualization Toolkit (VTK) served as middleware from the simulation results to the Mobile AR. Users could explore data intuitively through slicing, clipping, and manipulating the FEA results and realize AR-assisted interactive analysis with model modification. In this study, a 3D input device was created as interaction tools for data input and system control. In previous studies, augmented visualizations for FEA always requires implementations of additional devices (e.g., AR device screens and 3D input devices). Users are not allowed to have direct and natural interactions between virtual and physical environments, which will reduce the immersive experience to a certain extent. Interactions between virtual-physical environments still needs to be improved. It is noteworthy that recent developments and engineering applications of MR technology have shown that augmented visualization of FEA could facilitate gesture interaction, thereby enhancing the immersive experience of virtual-real interaction. Xu et al. [45] used the Visualization Toolkit (VTK) as a middleware to present the pre-calculation FEA results generated by MATLAB in HoloLens 2 to realize a virtual review application of FEA deformation results with a strong sense of immersion. And users can control the virtual objects of FEA deformation results through gesture interaction. Poh et al. [46] developed a mixed-reality interface to enhance the FEA workflow by allowing users to apply load parameters to the model surface in the form of gestural interactions. The proposed method enhanced engineers' understanding of the FEA from a MR interaction perspective.

2.3. State-of-the-art MR applications in the AEC industry

Mixed Reality (MR) technology has potential and value for application in the architecture, engineering, construction, and operation (AECO) industry (Cheng et al. [47]). HoloLens is one of the common MR devices. Logg et al. [48] presented a mixed-reality application which allows a user to define a physical problem governed by Poisson's equation and view the numerical solution superimposed on the real world. Du et al. [49] researched indoor navigation using HoloLens, showing that a self-centered perspective can improve pathfinding efficiency, reduce cognitive load, and enhance spatial awareness. Logg et al. [50] developed a mixed-reality application called HoloFEM to define and solve physical problems governed by partial differential equations

in real-world surroundings and demonstrated the application of augmented reality simulation to the time-dependent advection-diffusion equation. It is worth mentioning that all computations were carried out on the HoloLens device in this study. Malek and Moreu et al. [51,52] developed a new crack characterization algorithm toward real-time implementation standalone deployment for HoloLens and proposed a new methodology that enables a standalone real-time crack detection system for field inspection through HoloLens. In this study, both crack identification and information visualization were implemented in a standalone HoloLens. In the field of infrastructure monitoring, Al-Sabbag and Yeum et al. [53] created an interactive structural defect visual inspection system named XRIV, which is based on the HoloLens device and incorporates an interactive segmentation algorithm. For remote infrastructure inspections, data visualization interfaces and human-machine interaction are also important [54]. Existing research suggests that MR devices (e.g., HoloLens) integrate computing power and visualization modules that allow for in-situ data processing and presentation, somewhat avoiding the data transfer process.

MR also emphasizes the integration and merging of both physical reality and virtual reality (Rauschnabel et al. [55]). The calibration and synchronization of physical and virtual environments are crucial for the application of digital transformation in the construction industry [56]. Li et al. [57] innovatively proposed a method using the built-in depth camera of an HMD (i.e., HoloLens) to compare depth maps of the physical and virtual worlds. This approach evaluates misalignments, preventing assembly errors and improving operational efficiency. Dan et al. [14] designed and developed HoloDesigner, a mixed reality tool that combines virtual three-dimensional (3D) models with real-world environments for visualization and interaction, and they provided new insights into supporting on-site design work. Fukuda et al. [58] innovatively integrated semantic segmentation from deep learning into an MR system, enabling the evaluation and visualization of future landscape designs in real scenes through a blend of virtual and physical elements. Moreu et al. [59,60] developed a new, human-centered interface that gives inspectors real-time access to actionable structural data during inspection and monitoring enhanced in a virtual-physical calibration environment by HoloLens. This interface could provide a channel for direct sensor feedback while increasing awareness of reality to reduce gaze distraction. Yeum et al. [61] developed a system known as HMCI by integrating MR technology with a robotic data collection platform. This system allows for real-time spatial alignment between robots and MR head-mounted devices, thereby enhancing human-machine collaboration in infrastructure inspections. Wu et al. [62] integrated Digital Twin (DT), Deep Learning (DL), and Mixed Reality (MR) technologies into a newly developed real-time visual warning system. In this paper, virtual hazardous area markers are superimposed in situ at full size onto large-scale physical scenarios to construct an interactive virtual-physical merging environment, which enables construction workers to determine their safety status and avoid accidents proactively. Moreover, an interactive mixed reality environment that blends virtual and physical elements promoted teaching in the AEC industry. It helped enhance students' practical skills, preparing them for future work in the construction sector [63]. MR achieves virtual-physical environments merging by spatial anchors, which do not require additional physical markers and thus allow for virtual-physical calibration in large-scale scenes [64]. At the same time, holographic virtual content is locked directly into the physical environment under spatial anchors, with spatial interactions such as occlusions and collisions [65].

Through calibration and interaction between virtual-physical environments, MR is also a visualization technique that can enhance immersive experience and improve visual perception (Khaled et al. [66] and Kim et al. [67]). Prabhakaran et al. [68] reviewed and synthesized the existing research evidence through a systematic review to gain a better understanding of the state-of-the-art immersive technology

application in the architecture and construction sector. By examining the electrical construction field, Chalhoub et al. [69] explored MR's influence on the productivity and quality of electrical conduit construction, and they found that MR could significantly enhance industry practitioners' perception of electrical construction content through immersive experience. MR mainly relies on gestures to realize interactions in virtual and real environments, which are more direct and natural, and are useful for creating immersive experiences and enhancing the perception of engineered systems.

2.4. Summary

An overall conclusion of the literature review is shown in Fig. 1. In section 2.1, The paper begins with a relevant literature analysis of the FEA applications for infrastructure structure, where the main challenges are (1) Requirements for external computing and processing devices, (2) Necessary data transfer processes, and (3) Unintuitive perception of engineering systems. To make the FEA visualization more intuitive and interactive, in section 2.2, this paper provides an overview of work related to augmented visualization for FEA, where the main challenges include (1) Separation of the FEA calculation module and visualization module, (2) Limited virtual-physical calibration and in-situ visualization and (3) Inadequate interaction between virtual-physical environments. To bridge the research gap mentioned above, in section 2.3, this paper analyses the MR applications in the construction industry. The advantages of MR mainly include (1) Integration of computing power and visualization modules, (2) Calibration and interaction between virtual-physical environments, and (3) Enhanced immersive experience and perception. These advantages will compensate for the limitations mentioned in Sections 2.1 and 2.2 and, at the same time, can generously support this paper to establish the MR-enabled standalone real-time finite element analysis system for in-situ observation and calibration for structure safety diagnosis.

The remaining parts of this paper are organized as follows. The framework is proposed, and the related theoretical background is introduced in Section 3. Detailed steps for system implementation are given in Section 4. The results and discussions of the methodology are in Section 5. The conclusion and the perspective for future development are provided in Section 6.

3. Framework and related theoretical background

This paper proposed a framework for in-situ observation and calibration for structure safety diagnosis through integrated use of FEA and MR (see Fig. 2). The proposed method contains 2 modules, the offsite module, and the in-situ module. The offsite module primarily pertains to the preliminary work for developing this MR system, encompassing structural components in physical reality and virtual reality. For structural components in physical reality, this part mainly consists of spatial details data acquisition. Global Navigation Satellite System (GNSS) and three-dimensional (3D) terrestrial laser scanning (TLS) are employed for reconstructing 3D point clouds of structural components, providing a

comprehensive means of acquiring component data. Parameter estimation is carried out based on the 3D point clouds, enabling acquisition of geometric parameters, boundary conditions. For structural components in virtual reality, in this part, the preprocessing, computation, and post-processing modules of the finite element analysis were developed within the Unity Engine. Attribute sets are extracted for parameter estimation by deconstructing structural components. Explicit FEA theory is embedded, and virtual structural components are created as the FEA carrier based on Unity engine. Rendering mechanism is designed for visualization of components with FEA results. The in-situ module relates to the on-site application of this MR system. For structural components in mixed reality, the estimated parameters obtained from the structural components in physical reality will be utilized to update the Finite Element (FE) calculation model developed from the structural components in virtual reality through the holographic input interface. Then, the MR device (i.e., HoloLens 2) performed standalone FEA computing and in-situ visualization and calibration of FEA results to support onsite observation for structure safety diagnosis.

3.1. Requirements analysis for field structural safety diagnosis

Structural safety diagnosis is discovering physical and functional deficiencies, evaluating the safety of the structure and the causes of those deficiencies, and proposing methods of repairing and reinforcing those deficiencies so that appropriate measures can be taken on time (Ham et al. [70]). However, conventional visual inspections are always subject to engineering knowledge and field experiences and could hardly examine structure risks under as-is conditions. Not only that, but structural state data is required to determine the condition of structural safety and identify defects in a short time for field structural safety diagnosis (Ham et al. [70]). FEA tools and model updating algorithms could help represent the structural mechanical conditions and examine changes of stress and displacements under extreme environmental conditions according to the discovered structure defects and spatial changes. Thus, for field structural safety diagnosis, it is crucial and highly demanded to implement and obtain relatively accurate finite element analyses characterizing the main structural states (e.g., stresses) in a short time.

However, existing construction sites rarely have sufficient computational resources and stable and fast network transmission conditions. To establish a robust, timely, and reliable in-situ finite element analysis system, it is thus necessary to simplify the finite element model and integrate the computational and visualization modules of FEA into lightweight MR devices that can be flexibly used on-site.

3.2. Methods for capturing spatial details of in-service structures

3D TLS technology has recently been commonly used in the field of civil engineering for monitoring in-service engineering structures [71,72]. TLS has the advantages of large area, high resolution, and fast access to data information (e.g., Cartesian coordinates (x, y, z)) of the object, and can rapidly reconstruct a 3D point cloud model [73] of local

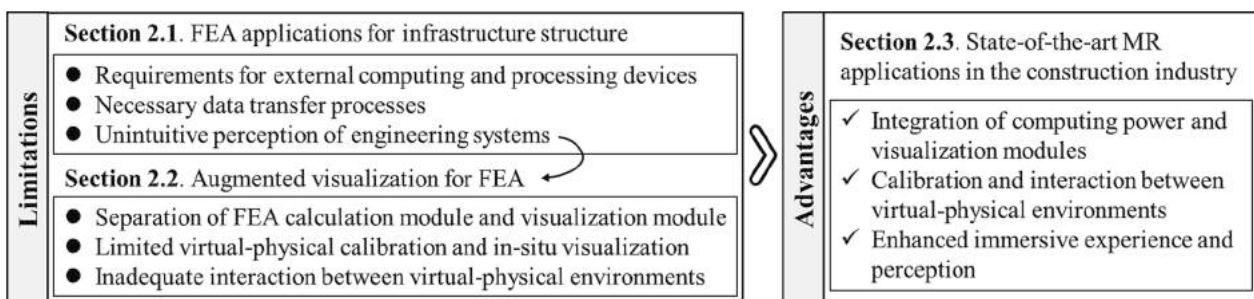


Fig. 1. Overall conclusion of the literature review.

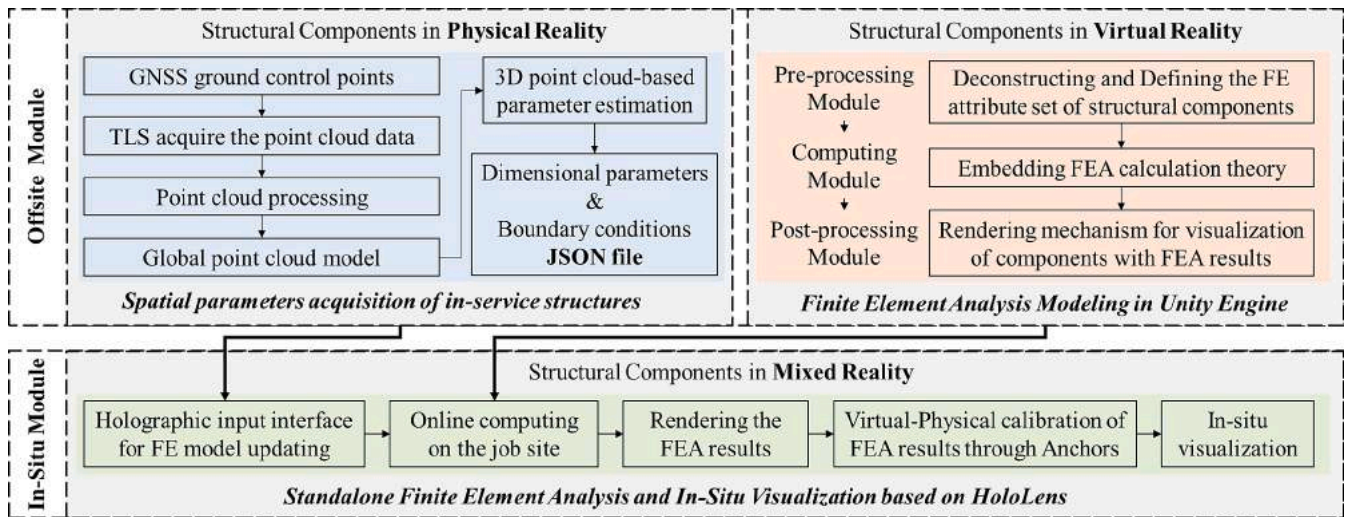


Fig. 2. A Framework for In-Situ Observation and Calibration for Structure Safety Diagnosis through FEA and MR.

target area in the independent coordinate system. Both the laser reflection intensity and 3D coordinates value of each point from TLS measurement are recorded with grid pattern guided laser beams, embodying the 3D surface geometry parameters (e.g., dimensional data) of the engineering structure. GNSS can provide precise position information (e.g., latitude, longitude, and altitude) to ground receivers in a global coordinate system.

In this paper, 3D TLS technology is used to obtain geometric data information of engineering structural components. Methods for capturing spatial details of in-service structures is shown in Fig. 3. GNSS is firstly used to collect ground control points (GCPs) in the site and record their coordinates. Then a 3D laser scanner is used to acquire the point cloud data in the site and GCPs will be labelled in the point cloud data. Additionally, the collected point cloud data need to be smoothed by using point cloud processing software (e.g., open-source software CloudCompare [74]) to remove the invalid points or noise points. Then the point cloud data will be registered with the corresponding GNSS GCPs through the labelled GCPs based on aligned algorithms [75] such as ICP (Iterative Closest Point) through CloudCompare. The alignment errors will be checked. Then all local point clouds will be uniformly

registered according to the GCPs to form a point cloud model in the global coordinate system.

A structural model can be one-dimensional, two-dimensional, or three-dimensional. This study utilizes a geometry-based feature extraction approach that enables voxelization and meshing of three-dimensional point cloud models obtained through TLS (for more details, see [76]). First, the global point cloud data is voxelized, converting the point cloud data into a voxel grid. This transforms the irregularly spaced points in the point cloud into a structured format, simplifying subsequent geometric analysis applications. Secondly, geometric features are extracted using methods such as corner and edge detection, plane detection, and curvature analysis. Then, the identified features (e.g., corners, edges, planes, etc.) are connected with lines or surfaces for mesh processing, creating a mesh representation of the point cloud that represents the original shape and structure of the scanned object. Finally, the mesh and extracted features are used to estimate the dimensional parameters of structural components (such as length, width, height, and volume) and assess boundary conditions. This approach can efficiently acquire the spatial parameters of in-service engineering structures.

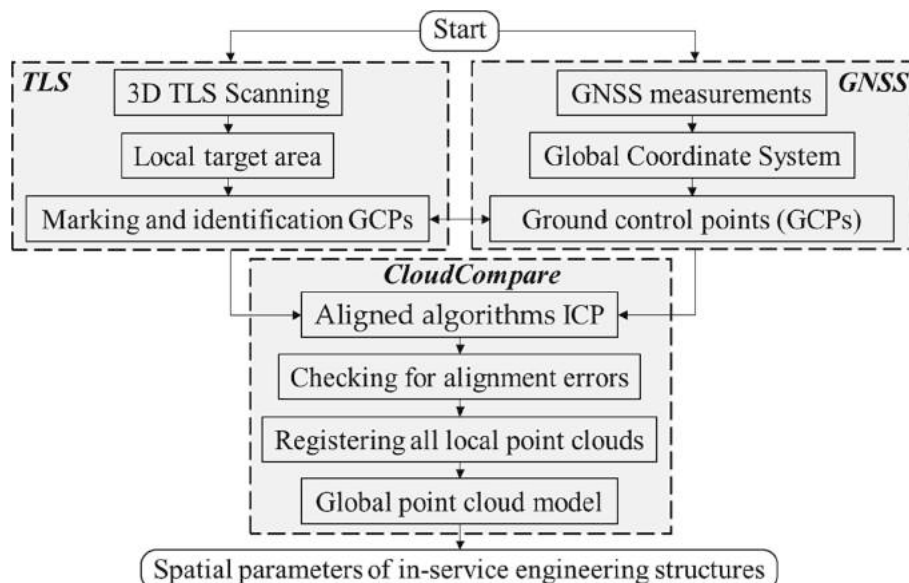


Fig. 3. Flowchart for spatial parameters acquisition of in-service structures with TLS and GNSS.

3.3. Theory for finite element analysis

3.3.1. Pre-processing for finite element analysis

To accurately create virtual structural components in a MR environment, in this study we propose the use of a structural component attribute set (Fig. 4) to deconstruct the structural components. In this study, we analyze the real structural components from the perspective of their ontological attributes and variable states and divide the set of attribute parameters for the real structural components into ontological parameters and state parameters. Virtual components in MR are created by defining the attribute set that can be used as a reference to represent the real structural components fully. The research object of this study is the FEA of structural components, so the pre-processing part of the FEA software is appropriately referred to when defining the attribute set.

According to the characteristics of the research object of this study, the attribute set was divided into ontological parameter set and state parameter set. The ontological parameter set contained geometric and material attributes and the state parameter set contained state attributes. Geometric attributes were mainly used to describe the shape and section geometric properties of structural components, divided into shape parameters and section geometric properties parameters: (1) The shape parameters included all the parameters that could describe the structural components' shape. We analyzed the most common rectangular structural components and divided the shape parameters into length, width, and height. According to the characteristics of the structural components, the length parameters could be divided into section length, calculated length, etc. The width parameters could be divided into section width, flange plate width, etc. The height parameters could be divided into section height, web plate depth, etc. (2) The sections' geometric properties parameters mainly included those that impacted the bearing performance of structural components. The proposed method considers the common parameters, such as static moment, centroid of area, product of inertia, polar moment of inertia, axial moments of inertia, principal axes of inertia, etc. Material attributes are mainly used to describe the physical properties of real structural components, which directly determine the response of structural components to environmental changes. The material attributes parameters used in this study include the elastic modulus, shear modulus, Poisson's ratio, mass density, and thermal conductivity.

The state attributes were mainly used to describe the state of the real structural components. In this study, we mainly divided state attributes into boundary condition parameters and load parameters: (1) The boundary conditions describe the constraints of the real structural components and are the necessary prerequisites for the solution of the FEA. According to the structural components' characteristics, in this study we divided the boundary conditions into two ends of solid support, two ends of simple support, one end of solid support, and one end of simple support. (2) Furthermore, we divided the loads into uniformly

distributed loads, concentrated loads, etc. Each load had a magnitude and position. It should be noted that, since the object of study was a single engineering component, parameters such as the connection relations and interaction relations between components were not considered in the definition of the attribute set.

3.3.2. Computing for finite element analysis

The proposed method uses the FEA theory as the mechanism calculation engine to guide the online real-time FEA calculation of virtual structural components. The core idea of finite element analysis is to construct a trial function using a segment splicing method for piecewise function approximation in a complex geometry domain, and then describe the whole complex geometry domain. The method used for constructing the mechanical balance equations, geometrical equations, and physical equations for the analytical solution by the principle of elasticity mechanics could clarify the calculation of the mechanism of stress and displacement in each direction. This paper aims to take advantage of the powerful fusion of mixed reality technology to enhance the interactivity between finite element analysis and real-time state parameters of structural critical components based on traditional structural state assessment methods, giving engineers the chance to conduct timely assessments of actual engineering structural critical components alongside finite element analysis on the job site.

However, in order to meet the requirements for rapid implementation and the relatively accurate FEA and to verify the rationality of the concept, while considering the limited computing power of MR devices (Malek and Moreu et al. [52]), this paper adopts a planar problem (two-dimensional structural model) with minimal arithmetic power requirement in finite element analysis and combines it with mixed reality technology for prototype development and verification. So, in this paper, the rectangular civil engineering critical components could be simplified according to the parameters of the attribute set of structural components.

Simplifying the three-dimensional finite element analysis to a two-dimensional plane will neglect the torsional effects, shear deformation effects, three-dimensional stress distribution, and three-dimensional effects of boundary conditions of the structural components. However, this paper takes rectangular civil engineering critical components as the research object, and the impact analysis is as follows: (1) Torsional effect: The components discussed in this paper belong to regular section components. They have relatively high torsional stiffness. When subjected to torque, their torsional deformation is relatively small, and the torsional effect is not significant. Therefore, neglecting the torsional effect is reasonable. (2) Shear deformation effect: The shear span ratio is a parameter to evaluate the relative importance of shear deformation and bending deformation of a beam. The shear span ratio of the components discussed in this paper is relatively small, and the shear effect is not significant. Simplifying it to a two-dimensional plane problem is

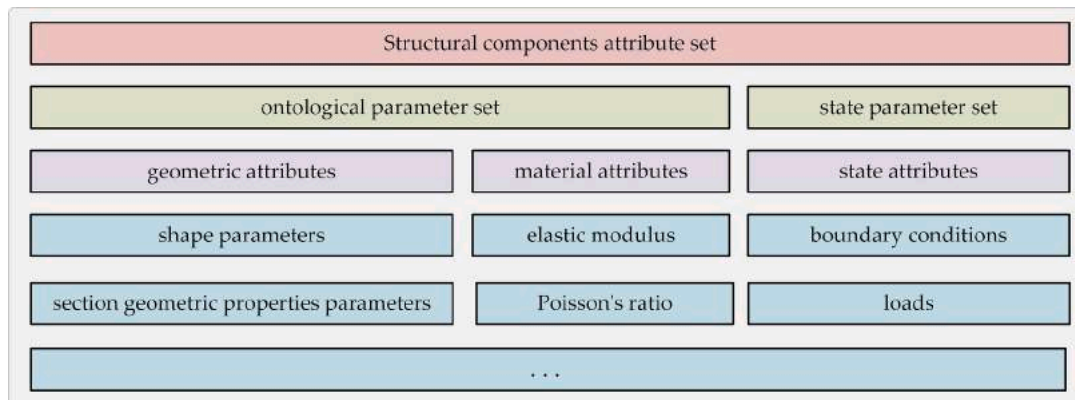


Fig. 4. The structural components attribute set.

reasonable. (3) Three-dimensional stress distribution: The three-dimensional stress distribution has a significant impact on thin-walled structures and hollow structures. However, the components discussed in this paper belong to solid structures, and their internal stress distribution is relatively uniform without obvious three-dimensional effects. Therefore, simplifying it to a two-dimensional plane problem will not introduce significant errors. (4) Three-dimensional effects of boundary conditions: The boundary conditions of the components discussed in this paper belong to the in-plane boundary conditions, and the three-dimensional effects of the boundary conditions have a small impact. Therefore, simplifying it to a two-dimensional plane problem is reasonable. In summary, this paper adopts a two-dimensional plane calculation method to replace the finite element analysis of rectangular civil engineering critical components, which can still well maintain the main state parameter characteristics of the structural components. At the same time, this simplification will greatly reduce the computational complexity and computational time, better adapting to the requirements for rapid and relatively accurate FEA for on-site field structural safety diagnosis.

4. System implementation

The system implementation of the method proposed is divided into three steps in total as shown in Fig. 5. The first step is spatial parameter acquisition. The point cloud model in the global coordinate system is acquired through the joint use of TLS and GNSS, and the spatial parameters of the structural components are obtained using parameter estimation methods. The second step is FEA modeling in Unity Engine. Virtual structural components are formed as FEA models by developing pre-processing, computing, and post-processing modules in the Unity engine. The third step is standalone FEA and in-situ visualization in HoloLens. The virtual structural components of the second step will be deployed in the HoloLens device in the form of HoloLens APPX. The user inputs the spatial parameters obtained in the first step in the holographic attribute parameter input interface to achieve the update of the FE model. Then, HoloLens calls the computing module in the second step for online computation and calls the post-processing module to render

the FEA results. Finally, the in-situ virtual-physical merging of the FEA results is achieved based on spatial anchors and gesture interaction to support in-situ observation and calibration of the structure safety diagnostics.

4.1. Spatial parameters acquisition of in-service structures

This paper employed the GNSS receiver and FARO 350S TLS scanner as shown in Fig. 6. The TLS scanner was used to perform 3D scanning of the critical structural components at the engineering site. CloudCompare (i.e., software for processing point cloud data) was used to perform point cloud registration of different control points. The open-source point cloud processing library, Point Cloud Library (PCL), was used to extract features and estimate parameters of the point cloud model of the critical structural components. Algorithm 1 outlines the main workflow for data acquisition and parameter estimation.

4.2. Finite element analysis modeling in Unity Engine

In this study, the authors used a virtual structural component based on Unity engine as an FEA carrier. The authors integrated the attribute set parameters of real components with the calculation theory of FEA and used spatial gridding chromaticity filling to present the physical mechanism. Fig. 7 shows the flow chart of finite element analysis modeling in Unity Engine to create simulated virtual structural components. This integrates the calculation and visualization modules of the FEA.

Pre-processing module. The attribute set was parameterized to realize the control of the virtual structural components. After obtaining the attribute set parameters of the structural components, the script was used to determine the calculation precision of the virtual structural components according to their scale. Drawing on the theory of finite element method, this script meshed the virtual structural components according to their precision and created basic prefabricated units of the corresponding scale in the Unity engine. The script calculated the coordinates of the center point of each grid cell of the virtual engineering component and assigned a basic prefabricated unit at the corresponding position. The script then substituted the center-point coordinates of the grid cell into the encapsulated mechanics mechanism to obtain the target calculated value before storing it in a new number set.

Computing module. More emphasis is placed on the implementability of in-situ structural condition diagnosis methods based on mixed reality and finite element analysis in engineering sites. Since this paper is mainly an experimental validation of the proposed method, the applicability of the proposed method was verified by simulating the variations in structural components' sizes and loads. The geometric data of structural components is obtained through parameter estimation based on 3D point clouds (section 4.1). Since the doubly clamped beams reinforcement is embedded in the walls at both ends. The concrete of the walls and beams is cast in place as a whole. As well as the stiffness of the walls at both ends is much greater than that of the beams. So, the boundary condition of the beams is determined as solid support at both ends. As a result, the analytical solutions used for finite element analysis are represented by Equations (1) - (4), which respectively correspond to the calculations for σ_x , σ_y , τ_{xy} , and Mises (i.e., σ_e). The material attribute properties used in the finite element analysis are those corresponding to an elastic behavior of concrete defined by Poisson's ratio $\nu = 0.29$. In this paper, a virtual load is employed to simulate the in-service state of a structure, and the stress is obtained through online calculation of HoloLens 2, assisting engineers in diagnosing the structural condition in situ.

$$\sigma_x = \frac{2ql^2}{h^3} (l^2 - 3x^2)y + \frac{4qy^3}{h^3} - \frac{3(2 + \mu)q}{2h} - \frac{\mu q}{2} \quad (1)$$

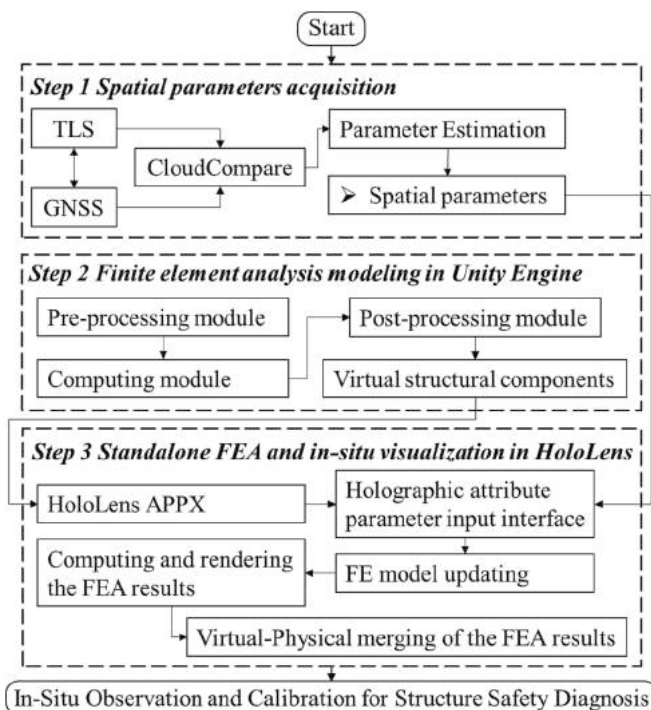


Fig. 5. The flow chart of system implementation.



Fig. 6. Spatial details data acquisition through TLS and GNSS.

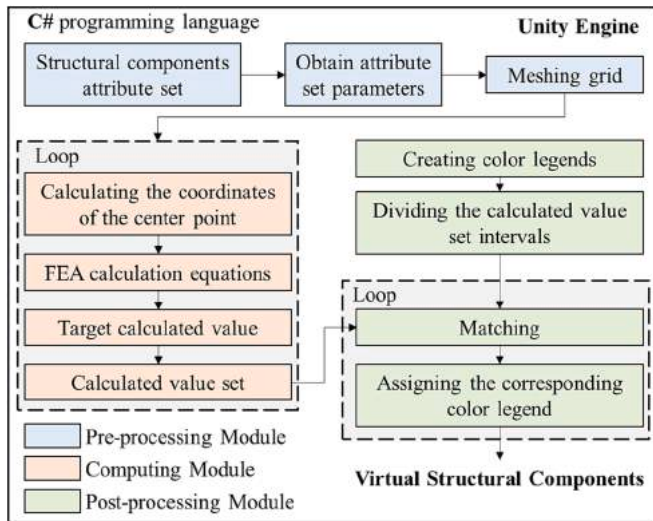


Fig. 7. The flow chart of finite element analysis modeling in Unity Engine.

$$\sigma_y = \frac{-2qy^3}{h^3} + \frac{3qy}{2h} - \frac{q}{2} \quad (2)$$

$$\tau_{xy} = \frac{6qxy^2}{h^3} - \frac{3qx}{2h} \quad (3)$$

$$\sigma_e = \sqrt{(\sigma_x + \sigma_y)^2 - 3(\sigma_x\sigma_y - \tau_{xy}^2)} \quad (4)$$

Post-processing module. The proposed method uses spatial gridding chromaticity filling as the mechanism presentation form to visualize the FEA results. Based on the calculation precision requirements, the script creates a certain number of color legends in the Unity engine and divides the calculated value set intervals according to the number of color legends created. The script then matches each calculated value with the divided calculated value intervals and assigns a corresponding color legend. Finally, the developed scripts are run in the Unity engine to create virtual structural components that are controlled by the attribute set.

4.3. Standalone finite element analysis and in-situ visualization based on HoloLens

4.3.1. Holographic attribute parameter input interface for FE model updating

In this study, we used a case of doubly clamped beam under uniform loads to validate the proposed method. In this paper, it is emphasized that the focus of this study is on verifying the validity of the proposed method, rather than on the accuracy of the finite element analysis. So, the doubly clamped beam can be simplified to a plane problem (section 3.3.2) for consideration according to the theory of elastic mechanics. Since the parameters of the attribute set (i.e., boundary conditions, load) were already partially defined by the doubly clamped beam under uniform loads, only the remaining parameters of the structural components in the attribute set needed to be defined. To comprehensively characterize the doubly clamped beam under a uniform load, we selected the length and height parameters in the geometric attribute set, the Poisson's ratio parameters in the material attribute set, and the load magnitude parameters in the state attribute set as the attribute variables (according to section 3.3.1.). Fig. 8 shows the human-machine holographic attribute parameter input interface developed in Unity 3D engine to obtain the parameter basis for creating virtual structural components.

To update the FE model, the Unity engine generates virtual structural components with ontological and state attributes, which include geometric, material, and state parameters. To begin with, the parametric model of the virtual structural component is defined. This paper presents an updated approach to the predefined virtual structural component model using the concept of instantiation through the holographic attribute parameter input interface. During the in-situ update of the FEA model, the geometric parameters are replaced with estimates based on the 3D point cloud, the material parameters are substituted with actual values of the structural components, and the state parameters are substituted with the boundary conditions described through parameter estimation in section 4.1.

During the actual execution of finite element analysis, users utilize mixed reality devices (e.g., HoloLens) to input spatial parameters acquired in the first step (Section 4.1) on a holographic attribute parameter interface, using gesture-operated virtual keyboards to update the FE model.

4.3.2. Computing and rendering the FEA results

The four buttons for σ_x , σ_y , τ_{xy} , and Mises on the right side of Fig. 8 package the C# scripts used to create the virtual structural components (for more details in section 4.2.) which were embedded the FEA

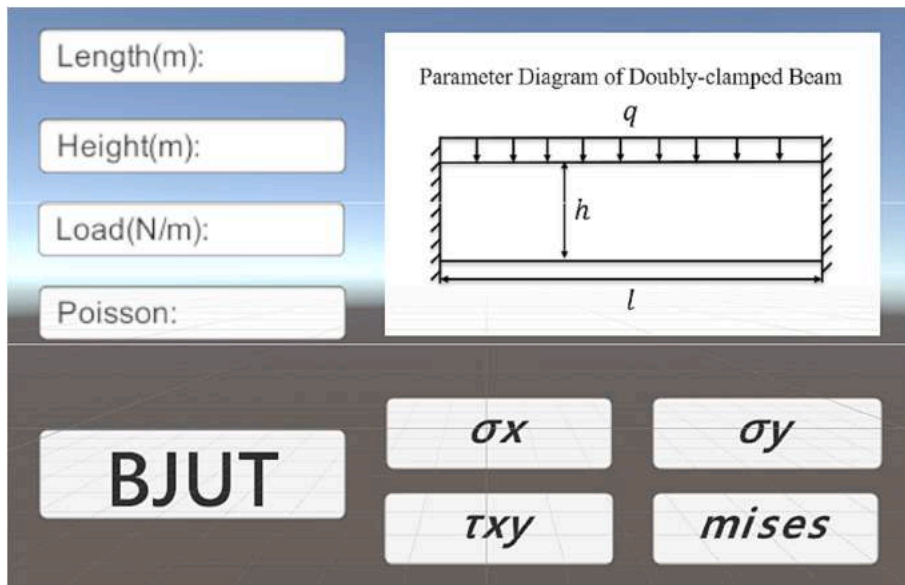


Fig. 8. The attribute parameter input interface.

computational theory. After the users enter the attribute parameter shown on the left side of Fig. 8, the attribute set of the virtual structural components are defined and the FE model is updated. By clicking the four buttons, users can create a virtual engineering component in an MR environment with the defined attribute set and perform online FEA calculations to obtain the corresponding stress nephogram (Fig. 9). When the calculation is completed, users can return to the parameter input interface by clicking the BJUT button to reupdate the FE model.

During the actual execution of finite element analysis, the primary task of mixed reality devices (e.g., HoloLens) in this step is to conduct real-time, online calculations using predefined finite element analysis programs (section 4.2.) based on actual parameters, generating corresponding finite element analysis data, which is then rendered online as a color nephogram.

4.3.3. Virtual-Physical merging of the FEA results through anchors

Mixed reality is a blend of physical and digital worlds, unlocking

natural and intuitive 3D human, computer, and environmental interactions. Mixed reality technology utilizes the built-in camera and sensors of a device to scan the physical world and generate a spatial map composed of meshes. The process of mixed reality virtual-to-real calibration places virtual assets in the physical world. Subsequently, a spatial anchor is created for the virtual assets by the mixed reality device to lock the virtual assets' position and rotation in the physical world. Thanks to the responsive gesture interaction module enabled by Mixed Reality technology, we developed some interactive functions (e.g., moving, scaling) with the help of the mixed-reality development toolkit (MRTK) to realize the virtual-to-real calibration and in-situ presentation of FEA results. The in-situ coordinates of the real structural components at the engineering site were used as the spatial anchor points for the MR presentation, as shown in Fig. 10. In this research, we superimposed the FEA results on the real structural components in the form of manual anchoring, avoiding the physical markers and additional interactive devices.

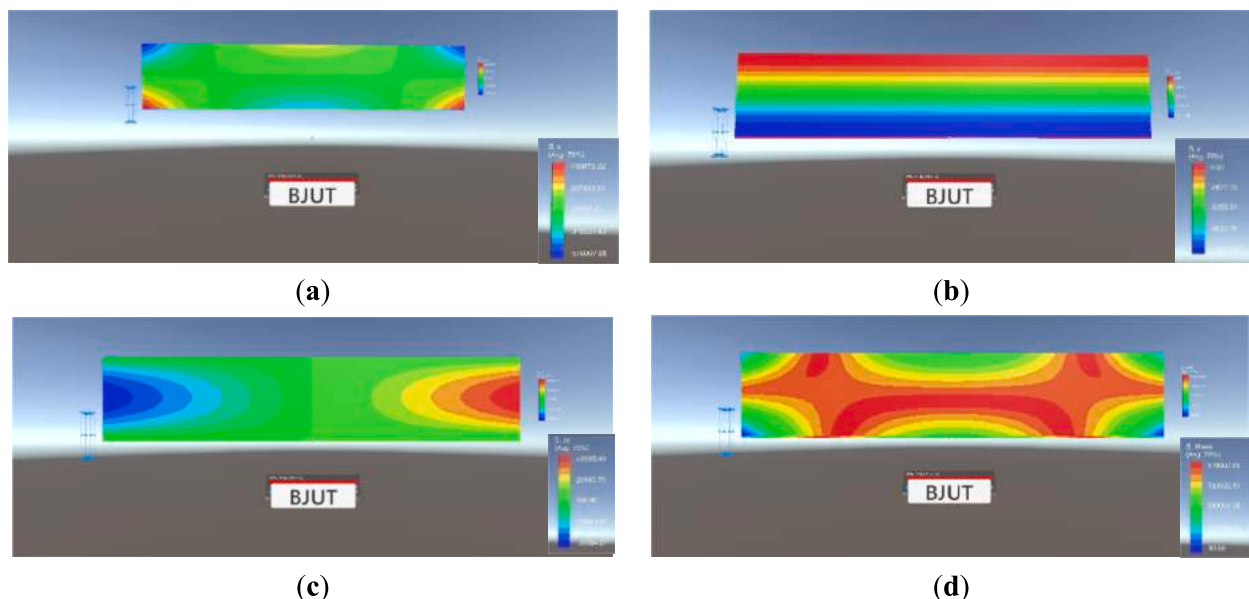


Fig. 9. Online calculation FEA results. (a) σ_x FEA results, (b) σ_y FEA results, (c) τ_{xy} FEA results, and (d) Mises FEA results.

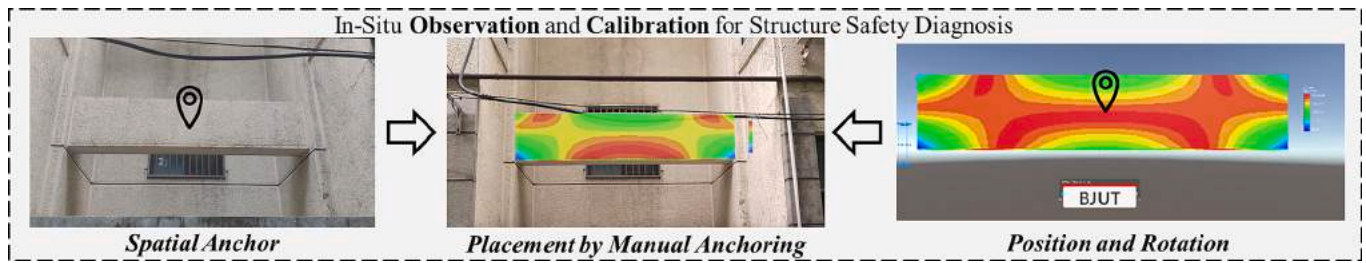


Fig. 10. Illustration of Virtual-Physical merging of the FEA results through Spatial Anchors.

4.4. Pseudo-code for MR application

The complete pseudo-code for MR application development is presented in Algorithm 1 and Algorithm 2. Algorithm 1 outlines the workflow for data acquisition and parameter estimation. The implementation pseudo-code for finite element analysis is presented in Algorithm 2. MR applications developed based on the above pseudo-code logic enable online computation of augmented finite element analysis for supporting onsite structure condition diagnosis.

Algorithm 1. Data acquisition and parameter estimation

```

Input: GNSS data and TLS data
Output: The dimensional parameters and boundary conditions of the structural components
GNSS workflow
1: gnsReceiver = new GNSSReceiver()
2: gnsReceiver.Configure()
3: gnsData = gnsReceiver.CollectData()
TLS workflow
4: laserScanner = new LaserScanner()
5: laserScanner.Configure()
6: pointCloud = laserScanner.Scan()
Data processing and registration
7: private ProcessData(GNSSData gnsData, PointCloud pointCloud)
8:   processedGNSSData = ProcessGNSSData(gnsData)
9:   processedPointCloud = ProcessPointCloud(pointCloud)
10:   registerData = RegisterData(processedGNSSData, processedPointCloud)
11: return registerData
Parameter estimation
12: private EstimateParameters(ProcessedData processedData)
13:   estimatedParams = Estimate(processedData)
14: return estimatedParams

```

Algorithm 2. C# scripts of finite element modeling and model updating

```

Input: structural components attribute set parameters (length, height, load, Poisson, etc.)
Output: Simulating and visualizing the structural dynamics of critical structural components
1: Using UnityEngine and UnityEngine.UI
2: Input [length, height, load, poisson]
Embedding FEA Theory
3: Function embeddingFEA(length, height, load, poisson)
4:   sigma [x, y, xy, mises] = Equation 1-4 (length, height, load, poisson)
5:   resultFEA = sigma [x, y, xy, mises]
6: return resultFEA
Creating the virtual structural components
7: Divide the structural components into grids and create a grid list A
8: Store list A as grid prefabs in Unity engine
9: For  $b_n < A$  do
10:   Calculate the structural dynamic stress of the grid points using Function embeddingFEA
11:   Store list B as the stress
12:   Update  $b_n$ 
13: End
14: Obtain the maximum and minimum values of stress from list B
15: Create material list C as the color legend
16: For  $c_n < C$  do
17:   Divide the stress interval according to list C
18:   Assign color material balls from blue to red depending on the interval to  $c_n$ 

```

(continued on next column)

(continued)

Algorithm 2. C# scripts of finite element modeling and model updating

```

19: Update  $c_n$ 
20: End
21: if Stress list B matches material list C then
22:   Assign material list C of the color legend to grid prefabs list A
23: End
FE model updating
24: Function modelupdating(length, height, load, poisson)
25:   Input = newInput[length, height, load, poisson]
26: return Input
27: End

```

5. Results

The feasibility of the proposed method for use in the integrated application of FEA and MR was verified in the context of a common fundamental civil engineering component (i.e., doubly clamped beam). With the analytical solution of the doubly clamped beam based on the elastic mechanics theoretical calculation mechanism, we used the C# language combined with the Unity 3D engine to carry out development validation and engineering field tests for the MR device (i.e., HoloLens 2).

5.1. In-situ observation and calibration for structure safety diagnosis

The developed application was deployed on the HoloLens 2 and engineering field tests were conducted using two different-sized doubly clamped beams in the No. 3 teaching building and No. 7 student dormitory building of Beijing University of Technology with different loads to verify the applicability of the proposed method.

The relevant parameters of the experimental verification are recorded in detail on the left side of Table 1. Calculations for both Group I and Group II were carried out based on the No. 3 teaching building to simulate a situation where the magnitude of the load on the structural components changes. Calculations for Group I and Group III were carried out in the No. 3 teaching building and No. 7 student dormitory building, respectively, to simulate a situation where there are structural components of different sizes. The results obtained from the online real-time FEA in HoloLens 2 under the corresponding attribute set parameters are recorded in detail on the right side of Table 1 and presented in the form of a colormap of the engineering field. The case validation of this paper is still in the experimental stage. However, in the practical application stage, to ensure the stress nephogram (by FEA embedded in MR device) is the same as the actual stress distribution (physical beams in the job site), the stress nephogram generated by the FEA program deployed on the mixed reality device must be compared with the stress sensor data at critical points on the physical beam to ensure that the errors are within acceptable limits.

Figs. 11 and 12 show the doubly clamped beams in the No. 3 teaching building and No. 7 student dormitory building from two different viewpoints, respectively. Figs. 13 and 14 show the user operation interface in HoloLens 2 from two different viewpoints, respectively. Figs. 15 and 16 show the in-situ presentation of the real-time FEA

Table 1
Relevant parameters and stress results used for field verification.

Groups	Attribute set parameters				Stress (Pa)				
	Length (m)	Height (m)	Load (N/m)	Poisson's Ratio	S11	S22	S12	Mises	
I	2.21	0.51	1000	0.29	Max	3690.75	0.00	3248.75	17,844.36
					Min	-17,844.36	-998.86	-3219.35	648.61
II	2.21	0.51	2000	0.29	Max	7381.50	0.00	6497.50	35,688.72
					Min	-35,688.72	-1997.72	-6438.70	1297.22
III	2.71	0.58	1000	0.29	Max	12,188.43	0.00	3504.31	25,608.96
					Min	-25,608.96	-996.51	-3478.45	59.61

*Stress results were all calculated online in real time using HoloLens 2 less than 1 sec (See Table 2).

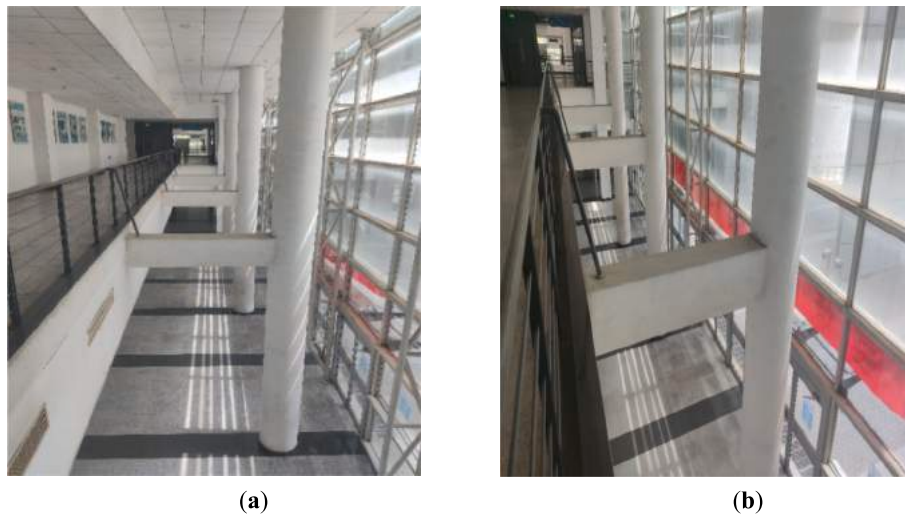


Fig. 11. Doubly clamped beams in the No. 3 teaching building: (a) viewpoint 1; (b) viewpoint 2.

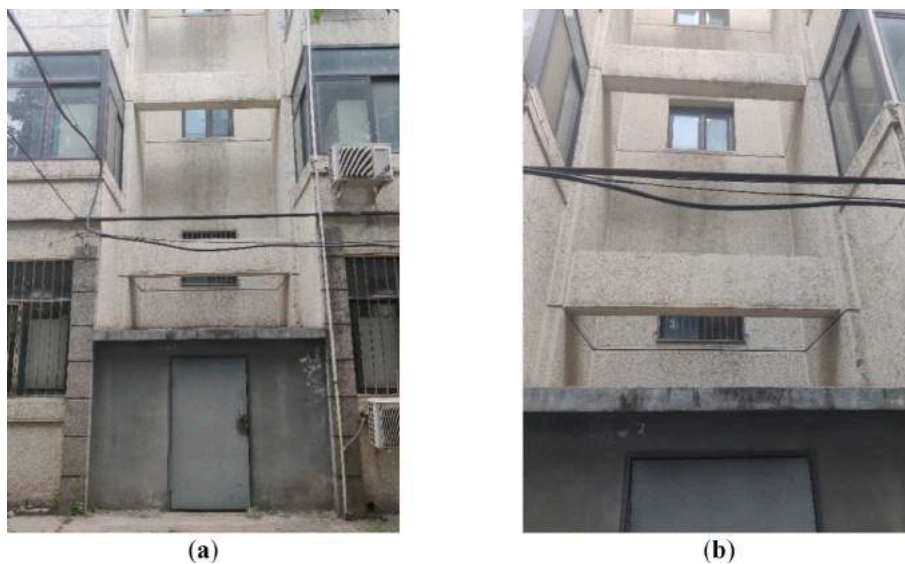


Fig. 12. Doubly clamped beams in the No. 7 student dormitory building: (a) viewpoint 1; (b) viewpoint 2.

calculation results obtained through the HoloLens 2 under the Group I and Group II attribute set parameters, respectively. Combined with the resultant data shown on the right side of Table 1, it can be seen from Fig. 15 and Fig. 16 that although the overall trends of the stress distribution are similar, the stress values found at the corresponding locations changed when the magnitude of the load applied to the structural components changed. The variation in stress is also reflected in the

colormap with stress value in Table 1 under different loads. Fig. 17 shows the in-situ presentation of the results of real-time FEA calculations through the HoloLens 2 under the Group III attribute set parameters. It can be seen through the real-time FEA calculations results obtained for Group I (Fig. 15) and Group III (Fig. 17) that the method proposed in this paper can be flexibly adapted to different sizes of components.



Fig. 13. The user interface in HoloLens 2: (a) the user interface at viewpoint 1; (b) the user interface at viewpoint 2.



Fig. 14. The user interface in HoloLens 2: (a) the user interface at viewpoint 1; (b) the user interface at viewpoint 2.

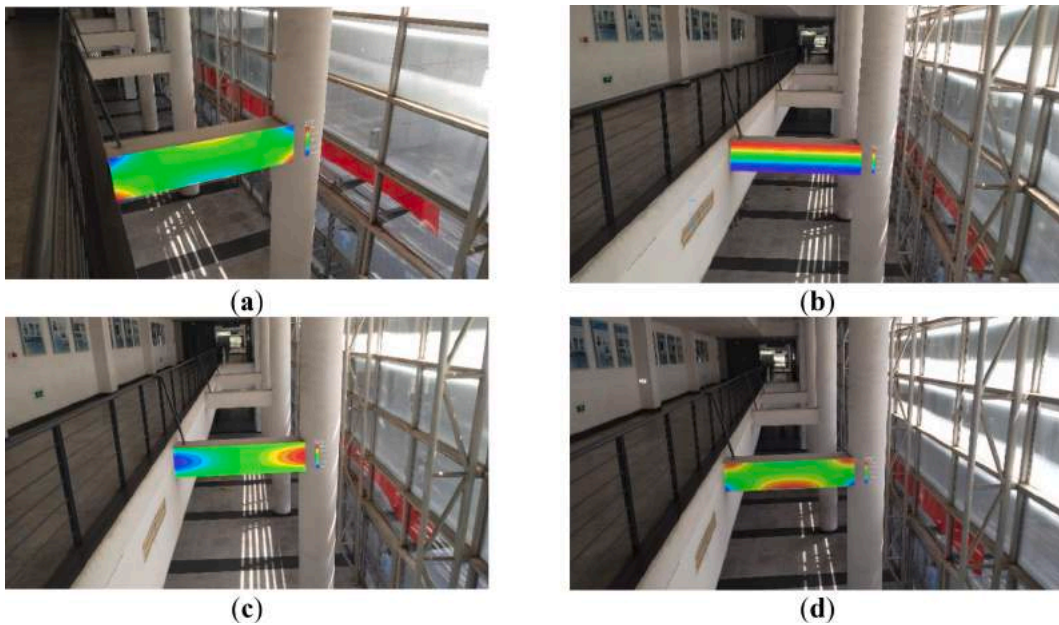


Fig. 15. FEA results obtained under the Group I attribute set parameters: (a) S11 FEA results; (b) S22 FEA results; (c) S12 FEA results; (d) Mises FEA results.

6. Validation and discussions

6.1. Validation

This paper rigorously evaluated the proposed MR-FEA system. It encompassed scalability validation across various structural components, a quantitative assessment of FEA result accuracy, and a performance analysis of the MR application implemented on the HoloLens 2 platform.

In this paper, the scalability of the proposed MR-FEA method for various structural components was demonstrated using a test case

involving a simply supported beam subjected to a uniformly distributed load. The method's adaptability across different component types was primarily facilitated by altering the computational equations within the module outlined in Section 4.2. This adaptation is explicitly detailed in the Embedding FEA Theory section (lines 3–5) of Pseudocode Algorithm 2. The FEA analysis of a simply supported beam subjected to a uniformly distributed load was conducted using equations (5)–(8). In the MR-FEA method, both the visualization module and the virtual-physical calibration module remained unchanged. Furthermore, as illustrated in Fig. 18, different FEA analysis types for basic structural components can be integrated into the MR attribute parameter input interface discussed

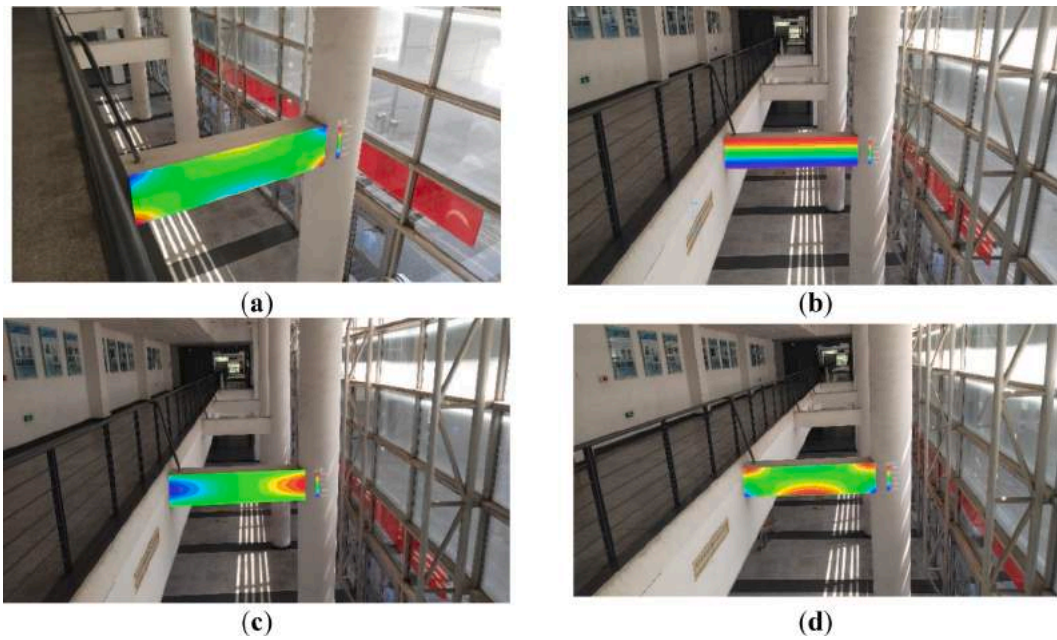


Fig. 16. FEA results obtained under the Group II attribute set parameters: (a) S11 FEA results; (b) S22 FEA results; (c) S12 FEA results; (d) Mises FEA results.

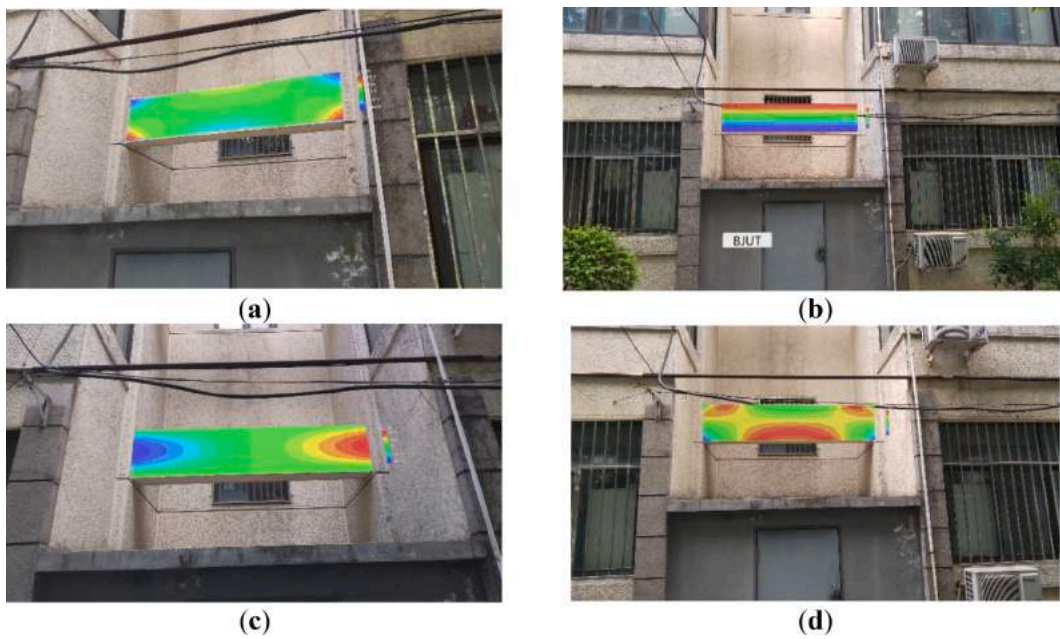


Fig. 17. FEA results obtained under the Group III attribute set parameters: (a) S11 FEA results; (b) S22 FEA results; (c) S12 FEA results; (d) Mises FEA results.

in Section 4.3.1. The *F-F B* button, depicted in Fig. 18(a), denotes the analysis type for a fixed–fixed beam under a uniformly distributed load. Similarly, the *S-S B* button, shown in Fig. 18(b), corresponds to the analysis of a simply supported beam under a uniformly distributed load. The selection of the analysis type can be toggled via these buttons. Consequently, the MR-FEA method introduced in this paper allows for the rapid transfer and integration of structural components under varying boundary conditions and loading states.

$$\sigma_x = \frac{-6q}{h^3}x^2y + \frac{4qy^3}{h^3} + \frac{6ql^2}{h^3}y - \frac{3q}{5h}y \quad (5)$$

$$\sigma_y = \frac{-2qy^3}{h^3} + \frac{3qy}{2h} - \frac{q}{2} \quad (6)$$

$$\tau_{xy} = \frac{6qxy^2}{h^3} - \frac{3qx}{2h} \quad (7)$$

$$\sigma_e = \sqrt{(\sigma_x + \sigma_y)^2 - 3(\sigma_x\sigma_y - \tau_{xy}^2)} \quad (8)$$

The simply supported beam is the typical bending member and one of the most fundamental components in civil engineering structures. This paper involved designing a mechanical experiment to validate the accuracy of the MR-FEA system’s computational results. This experiment featured a simply supported beam under a uniformly distributed load. The experimental beam’s geometric dimensions are 3.2 m in length, 0.4 m in width, and 0.8 m in height, with a concrete strength of C30. It was supported by bearings to constitute a simply supported system. The applied load was uniformly distributed across the beam

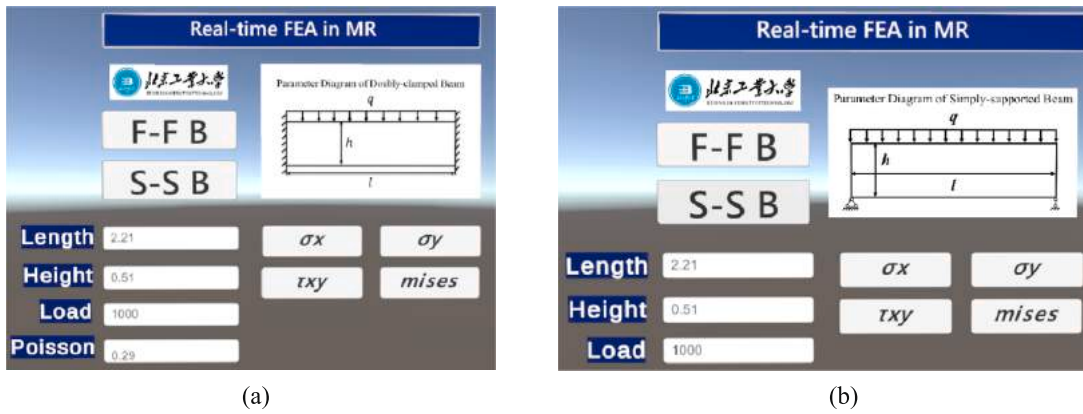


Fig. 18. Holographic interface integrating different FEA types. (a) Holographic interface of the F-F B button (b) Holographic interface of the S-S B button.

using weighted blocks. Five distinct loading conditions (Groups IV-IX) were established, corresponding to 622.5 N/m, 1245 N/m, 1867.5 N/m, 2490 N/m, 3112.5 N/m, and 3735 N/m, to replicate various loading scenarios. In the experimental setup, four critical points were identified on the beam at positions $h/6$ (K1), $h/3$ (K2), $2h/3$ (K3), and $5h/6$ (K4) from the top section. Mechanical sensors (i.e., concrete strain gauges) were deployed at these points, as shown in Fig. 19. During the experiment, a static testing system recorded the strain values at these critical points of the actual simply supported beam under various load levels. Then, the corresponding stress values at these points were calculated using the stress-strain conversion equation (i.e., equation (9)). Simultaneously, the MR-FEA system was applied in situ to overlay the computed stress cloud map with the experimental beam for virtual-physical calibration, as illustrated in Fig. 20. Fig. 21 presents a comparison between the actual beam stress, as measured by sensors at each critical point under various loading conditions, and the corresponding stress computed by the MR-FEA system. Additionally, the error between the sensor-measured stress and the MR-FEA system-derived stress was quantified using the error calculation equation (equation (10)), as depicted in Fig. 22. The observed error did not exceed 4.50 %, indicating a high level of accuracy. Such precision in finite element analysis is crucial for accurately characterizing the structural state and meets the requirements for finite element analysis applications in situ at engineering sites.

$$\sigma = E \times \epsilon \tag{9}$$

$$Error = \frac{|Value_{(Sensor)} - Value_{(MR-FEA)}|}{Value_{(MR-FEA)}} \times 100\% \tag{10}$$

This paper encapsulated the proposed method into an MR program based on the .NET framework utilizing Unity. The performance of the MR program was quantitatively analyzed in terms of the time required for FEA computation, the time for visualizing FEA results, and the average frames per second (FPS) during the MR application's operation. The *Stopwatch* class, part of the *System.Diagnostics* namespace in the .NET framework, was employed to precisely record the elapsed time from the initiation to the conclusion of a script. To assess the effectiveness of the proposed method, the *Stopwatch* class was utilized to separately measure the execution times of the computational and post-processing visualization modules within the MR program. Frame rate is often used as a standard to measure the smoothness of an application and is one of the key indicators in performance testing. In this paper, a Unity performance monitoring script was developed, leveraging the *Time.unscaledDeltaTime* property within the Unity engine. This property facilitated the acquisition of the duration of each preceding frame, enabling the calculation of the current real-time FPS. Moreover, the script calculates the average frame rate since the program's launch by recording the total number of frames and the cumulative total time during the program's operation. This approach comprehensively evaluated the program's efficiency and smoothness, thus effectively monitoring and gauging its performance. The related quantitative data are recorded in Table 2 (taking S11 as an

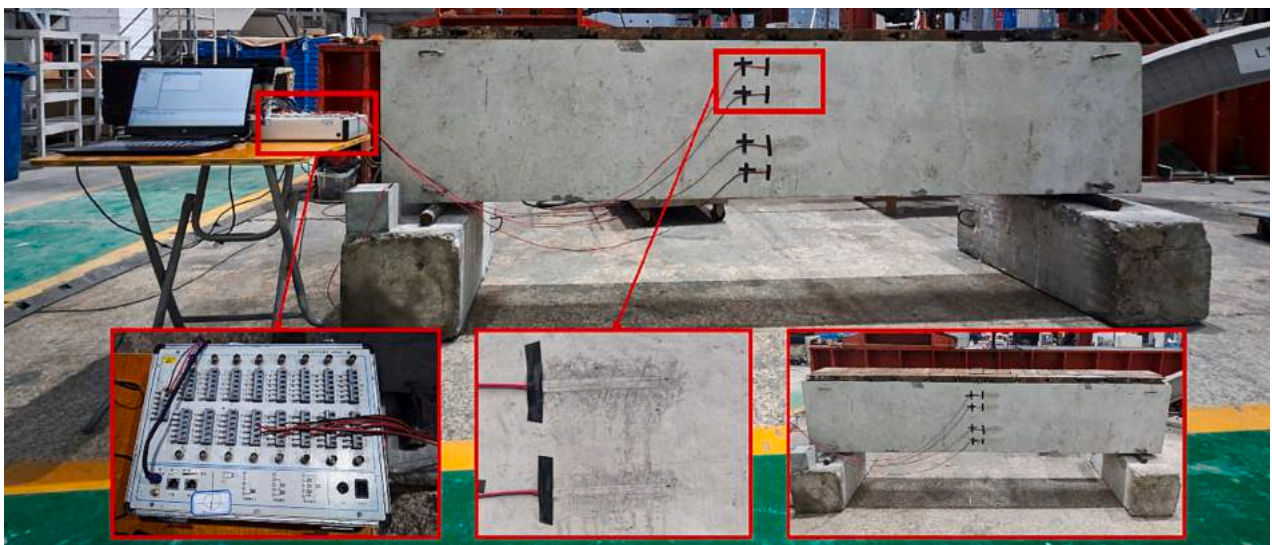


Fig. 19. Illustration of mechanical experiment for a simply supported beam under uniformly distributed load.



Fig. 20. In-situ application of the MR-FEA system.

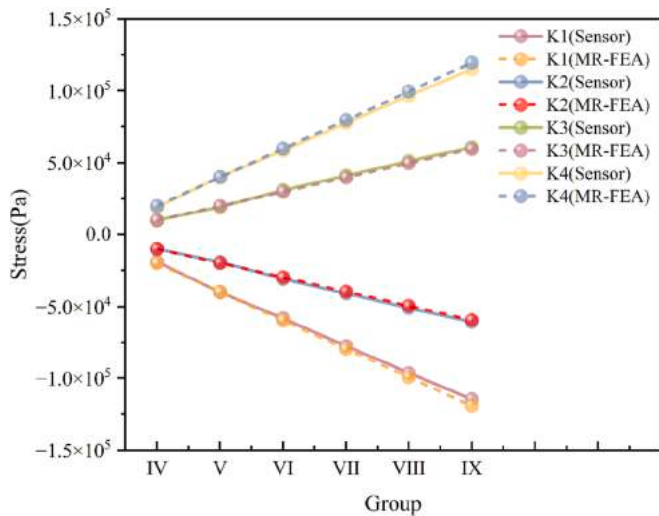


Fig. 21. Comparison chart of actual beam stress measured by sensors and beam stress calculated by the MR-FEA system.

example), where the computation time and visualization time are the average values from 10 independent runs of the MR program under the same conditions. To eliminate the impact of possible frame rate instability at the beginning of the program's launch on the evaluation, this paper sets the calculation interval for the average frame rate from the first to the second minute after the MR program starts. Similarly, this

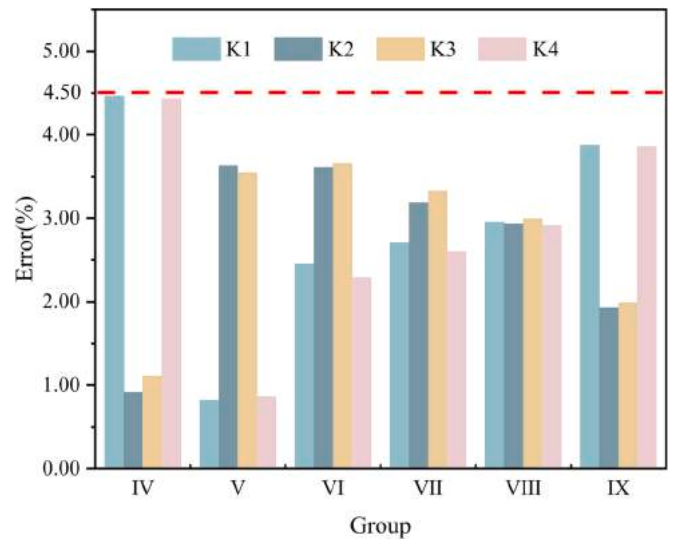


Fig. 22. Error of actual beam stress measured by sensors and beam stress calculated by the MR-FEA system.

average frame rate will be calculated based on data from 10 independent runs of the MR program. Table 2 demonstrates that 1) the more significant the component size, the greater the number of meshes required, resulting in longer visualization times; 2) the total computation and visualization times of the MR-FEA system approximate 1 s, satisfying the

Table 2
Quantitative analysis table of MR program performance.

Groups	Dimensions (m ²)	Load (N/m)	FEA in MR Calculation time (ms)	FEA in MR Visualization time (ms)	Average Frame Rate (FPS)
I	2.21 × 0.51	1000	0.7483	492.1713	60
II	2.21 × 0.51	2000	0.7451	434.8055	58
III	2.71 × 0.58	1000	1.0368	827.5530	59
IV	3.20 × 0.80	622.5	2.1808	1067.2813	55
V	3.20 × 0.80	1245	2.1555	937.3137	60
VI	3.20 × 0.80	1867.5	2.1260	1000.2681	56
VII	3.20 × 0.80	2490	2.1459	985.5084	56
VIII	3.20 × 0.80	3112.5	2.1227	1058.7705	58
IX	3.20 × 0.80	3735	2.1427	1023.5458	60

*For reference: A frame rate of 60 frames per second is typically regarded as comfortable for Mixed Reality applications on HoloLens 2 [77].

requirements for immediate finite element analysis calculations at engineering sites; 3) the MR-FEA system's average FPS exceeds 55, generally maintaining around 60, signifying high operational efficiency and smoothness of the program.

6.2. Discussions

Through the integrated development and engineering field tests of FEA and MR, we establish an MR-enabled standalone real-time finite element analysis system and realize the calibration and augmented visualization of finite element data in the virtual-physical fusion environment for intuitive observation and agile structural safety diagnosis. This study solves the challenges inherent in utilizing the FEA method, such as the fact that (1) requirements for external computing and processing devices and (2) necessary data transfer processes in traditional FEA, and that (3) traditional FEA has the disadvantages of unintuitive perception of engineering systems. We integrate the calculation and visualization modules of FEA based on MR without external computing devices. In this paper, we achieve the virtual-physical merging through the spatial anchor technology of MR devices (i.e., HoloLens), which avoids using physical markers and makes it more suitable for large-scale scenes at engineering sites. Meanwhile, the method proposed in this paper carries out parameter input and virtual-physical interaction through a holographic interface, eliminating the data transmission process and the use of external interaction devices. Thus, finite element analyses can be implemented and can obtain a relatively accurate characterization of the main structural stress states in a short time. Moreover, the implicit and invisible internal force status of the structure is calculated in situ and explicitly visualized. In other words, the MR-FEA system enhances human visual capabilities, enabling an intuitive visual perspective of the internal force states within the engineering structures system.

However, limitations still exist. For instance, (1) this study only focuses on integrating mixed reality and finite element analysis applications for critical structural components, the accuracy and timeliness of parameter acquisition still need to be improved when using manual input based on the mixed reality interactive interface to acquire state parameters; (2) for structural components with irregular and complex geometric shapes, it is difficult to create virtual structural components by changing the parameters of the component attribute set; and (3) the finite element analysis mechanisms used in this paper are all computational models for critical structural components with no damage and cannot cover the components that have been damaged internally in actual engineering projects.

7. Conclusion and future work

In this study, the authors proposed an in situ real-time FEA of critical structural components that integrates FEA and MR. The authors used MR

combined with engineering intrinsic mechanisms for online analysis to simulate, evaluate, and visualize the structural dynamics of critical structural components, expanding the application of MR in the engineering field and providing new ideas for the integrated application of FEA and MR.

Future research directions include: (1) with the use of sensors to capture stress changes inside critical structural members, the sensor information also needs to be integrated, processed, and applied based on mixed reality devices to ensure the timeliness and accuracy of the actual component parameter acquisition; (2) the real-time modeling of structural components with irregular and complex geometric shapes using mesh data of target objects generated by real-time scanning in HoloLens 2; (3) proven structural defect detection methods (e.g., ray detection and laser ultrasonic detection methods) and FE model update methods (e.g., machine learning) can be used to enrich the mechanistic computation engine and enhance the adaptability of interactive finite element analysis for structural condition assessment of engineering components based on a mixed reality environment.

CRedit authorship contribution statement

Xuefeng Zhao: Supervision, Funding acquisition, Conceptualization. **Wangbing Li:** Writing – original draft, Methodology. **Zhe Sun:** Writing – review & editing, Software. **Meng Zhang:** Validation. **Lingli Huang:** Validation.

Declaration of competing interest

The authors declare that they have no known competing financial interests or personal relationships that could have appeared to influence the work reported in this paper.

Data availability

Data will be made available on request.

Acknowledgements

This work was funded by the sub-committee of teaching guidance for engineering management and engineering costing of The Ministry of Education of The People's Republic of China, grant number CMPC202129.

References

- [1] L. Perumal, D.T.T. Mon, Finite Elements for Engineering Analysis: A Brief Review, in: Proceedings of the Modeling, Simulation and Control, Singapore, 16 September 2011, pp. 60–68.
- [2] A. Boccaccio, A. Ballini, C. Pappalettere, D. Tullo, S. Cantore, A. Desiate, Finite Element Method (FEM), Mechanobiology and Biomimetic Scaffolds in Bone Tissue Engineering, *Int. J. Biol. Sci.* 7 (2011) 112–132, <https://doi.org/10.7150/ijbs.7.112>.
- [3] M. Negru, I. Georgescu, E. Albota, Optimization of a large steel truss structure used in civil engineering, by Finite Element Method, in: Proceedings of the Finite Differences, Finite Elements, Finite Volumes and Boundary Elements, Wisconsin, United States, 11–13 September 2008, pp. 70–73.
- [4] J.M. Huang, S.K. Ong, A.Y.C. Nee, Visualization and interaction of finite element analysis in augmented reality, *Comput.-Aided Des.* 84 (2017) 1–14, <https://doi.org/10.1016/j.cad.2016.10.004>.
- [5] G. Iskander, E. Soliman, E. Sayed-Ahmed, Design of built-up steel beam-columns composed of two-channel sections, *Can. J. Civ. Eng.* 48 (2021) 1508–1522, <https://doi.org/10.1139/cjee-2020-0151>.
- [6] A. Cancelli, S. Laflamme, A. Alipour, S. Sritharan, F. Ubertini, Vibration-based damage localization and quantification in a pretensioned concrete girder using stochastic subspace identification and particle swarm model updating, *Struct. Health Monit.-Int. J.* 19 (2020) 587–605, <https://doi.org/10.1177/1475921718820015>.
- [7] Trappey, J.C. Amy, et al., How to manage and balance uncertainty by transdisciplinary engineering methods focusing on digital transformations of complex systems, *Advanced Engineering Informatics* 59 (2024) 102330. <https://doi.org/10.1016/j.aei.2023.102330>.

- [8] Fan Li, et al., Immersive technology-enabled digital transformation in transportation fields: a literature overview, *Expert Syst. Appl.* 202 (2022) 117459, <https://doi.org/10.1016/j.eswa.2022.117459>.
- [9] Ching Hung Lee, et al., Design and management of digital transformations for value creation, *Advanced Engineering Informatics* 52 (2022) 101547. <https://doi.org/10.1016/j.aei.2022.101547>.
- [10] Shohin Ahleroff, et al., Digital twin as a service (DTaaS) in industry 4.0: An architecture reference model, *Adv. Eng. Inform.* 47 (2021) 101225, <https://doi.org/10.1016/j.aei.2020.101225>.
- [11] Dongli Gao, Eric Wai Ming Lee, Yiu Yin Lee, The influence of context effects on exit choice behavior during building evacuation combining virtual reality and discrete choice modeling, *Advanced Engineering Informatics* 57 (2023) 102072. <https://doi.org/10.1016/j.aei.2023.102072>.
- [12] Get Started with Mixed Reality. Available online: <https://docs.microsoft.com/en-us/windows/mixed-reality/discover/get-started-with-mr> (accessed on 19 May 2022).
- [13] J. Miller, M. Hoover, E. Winer, Mitigation of the Microsoft HoloLens' hardware limitations for a controlled product assembly process, *Int. J. Adv. Manuf. Technol.* 109 (2020) 1741–1754, <https://doi.org/10.1007/s00170-020-05768-y>.
- [14] Y.Z. Dan, Z.J. Shen, J.Q. Xiao, Y.Y. Zhu, L. Huang, J. Zhou, HoloDesigner: A mixed reality tool for on-site design, *Autom. Constr.* 129 (2021) 103808, <https://doi.org/10.1016/j.autcon.2021.103808>.
- [15] S. Alizadehsalehi, A. Hadavi, J.C. Huang, From BIM to extended reality in AEC industry, *Autom. Constr.* 116 (2020) 103254, <https://doi.org/10.1016/j.autcon.2020.103254>.
- [16] P.F. Gouveia, J. Costa, P. Morgado, R. Kates, D. Pinto, C. Mavioso, J. Anacleto, M. Martinho, D.S. Lopes, A.R. Ferreira, et al., Breast cancer surgery with augmented reality, *Breast* 56 (2021) 14–17, <https://doi.org/10.1016/j.breast.2021.01.004>.
- [17] M.P. Strzys, S. Kapp, M. Thees, P. Klein, P. Lukowicz, P. Knierim, A. Schmidt, J. Kuhn, Physics holo.lab learning experience: using smartglasses for augmented reality labwork to foster the concepts of heat conduction, *Eur. J. Phys.* 39 (2018) 035703, <https://doi.org/10.1088/1361-6404/aaa8fb>.
- [18] M. Gheisari, B. Becerik-Gerber, C.S. Dossick, Emerging learning technologies for future of work and education in engineering, *Adv. Eng. Inf.* (2022) 101775, <https://doi.org/10.1016/j.aei.2022.101775>.
- [19] G.D. Dhadse, G.D. Ramtekkar, G. Bhatt, Finite element modeling of soil structure interaction system with interface: a review, *Arch. Comput. Meth. Eng.* 28 (2021) 3415–3432, <https://doi.org/10.1007/s11831-020-09505-2>.
- [20] F. Erdal, M.P. Saka, Ultimate load carrying capacity of optimally designed steel cellular beams, *J. Constr. Steel Res.* 80 (2013) 355–368, <https://doi.org/10.1016/j.jcsr.2012.10.007>.
- [21] I.S. Hoffman, B.M. Lazzari, A. Campos, P.M. Lazzari, A.R. Pacheco, Finite element numerical simulation of a cable-stayed bridge construction through the progressive cantilever method, *Struct. Concr.* 23 (2022) 632–651, <https://doi.org/10.1002/suco.202100662>.
- [22] H.V. Dang, M. Tatipamula, H.X. Nguyen, Cloud-based digital twinning for structural health monitoring using deep learning, *IEEE Trans. Ind. Inf.* 18 (6) (2021) 3820–3830, <https://doi.org/10.1109/TII.2021.3115119>.
- [23] A.M. Gharad, R.S. Sonparote, Study of direct finite element method of analysing soil-structure interaction in a simply supported railway bridge subjected to resonance, *Iranian J. Sci. Technol.-Trans. Civ. Eng.* 43 (2019) 273–286, <https://doi.org/10.1007/s40996-018-0139-7>.
- [24] Diz-Mellado Eduardo, et al., Non-destructive testing and Finite Element Method integrated procedure for heritage diagnosis: The Seville Cathedral case study, *J. Build. Eng.* 37 (2021) 102134, <https://doi.org/10.1016/j.jobe.2020.102134>.
- [25] S. Zhang, P.u. Huang, W. Yan, A data-driven approach for railway in-train forces monitoring, *Adv. Eng. Inf.* 59 (2024) 102258, <https://doi.org/10.1016/j.aei.2023.102258>.
- [26] F. Jiang, et al., Digital twin and its implementations in the civil engineering sector, *Automation in Construction* 130 (2021) 103838, <https://doi.org/10.1016/j.autcon.2021.103838>.
- [27] Su Shuaiming, et al., Digital twin and its potential applications in construction industry: state-of-art review and a conceptual framework, *Adv. Eng. Inform.* 57 (2023) 102030, <https://doi.org/10.1016/j.aei.2023.102030>.
- [28] Jiménez Rios, Alejandro, Vagelis Plevris, Maria Nogal, Bridge management through digital twin-based anomaly detection systems: a systematic review, *Frontiers in Built Environment* 9 (2023) 61. <https://doi.org/10.3389/fbuil.2023.1176621>.
- [29] T. Moi, A. Cibicik, T. Rølvåg, Digital twin based condition monitoring of a knuckle boom crane: An experimental study, *Eng. Fail. Anal.* 112 (2020) 104517, <https://doi.org/10.1016/j.engfailanal.2020.104517>.
- [30] H. Wang, et al., Real-time precision reliability prediction for the worm drive system supported by digital twins, *Reliab. Eng. Syst. Saf.* 109589 (2023), <https://doi.org/10.1016/j.res.2023.109589>.
- [31] S.K. Ong, J.M. Huang, Structure design and analysis with integrated AR-FEA, *CIRP Ann.* 66 (2017) 149–152, <https://doi.org/10.1016/j.cirp.2017.04.035>.
- [32] D. Mourtzis, Simulation in the design and operation of manufacturing systems: state of the art and new trends, *Int. J. Prod. Res.* 58 (7) (2020) 1927–1949, <https://doi.org/10.1080/00207543.2019.1636321>.
- [33] Dimitris Mourtzis, Design and operation of production networks for mass personalization in the era of cloud technology, Elsevier, 2021. <https://doi.org/10.1016/C2019-0-05325-3>.
- [34] M. Olbrich, A. Franek, D. Weber, Interacting with FEM Simulated Tubes in AR, *Lect. Notes Comput. Sci. (incl. Subser. Lect. Notes Artif. Intell. Lect. Notes Bioinform.)* 13095 (2021) 305–317, https://doi.org/10.1007/978-3-030-90963-5_23.
- [35] S. Dongwoo, E. Kim, J. Kim, Finite Element Analysis & Augmented Reality based Mechanical Product Simulation Platform for Small-Medium sized Enterprise Industry, *Adv. Sci. Technol. Lett.* 64 (2014) 26–30. <https://doi.org/10.14257/aslt.2014.64.07>.
- [36] D. Mourtzis, J. Angelopoulos, N. Panopoulos, Integration of Mixed Reality to CFD in Industry 4.0: A Manufacturing Design Paradigm, *Procedia CIRP* 107 (2022) 1144–1149, <https://doi.org/10.1016/j.procir.2022.05.122>.
- [37] D. Mourtzis, J. Angelopoulos, N. Panopoulos, Challenges and opportunities for integrating augmented reality and computational fluid dynamics modeling under the framework of industry 4.0, *Procedia CIRP* 106 (2022) 215–220, <https://doi.org/10.1016/j.procir.2022.02.181>.
- [38] D. Mourtzis, J. Angelopoulos, N. Panopoulos, in: *Integration of Mixed Reality (MR) and Structural Analysis towards Industry 4.0*, Springer International Publishing, Cham, 2022, https://doi.org/10.1007/978-3-031-17629-6_77.
- [39] M. Yavuz Erkek, S. Erkek, E. Jamei, M. Seyedmahmoudian, A. Stojcevski, B. Horan, Augmented reality visualization of modal analysis using the finite element method, *Appl. Sci.* 11 (2021) 1310, <https://doi.org/10.3390/app11031310>.
- [40] M.Z. Muthalif, D.S. Abdul, K. Khoshelham, A review of augmented reality visualization methods for subsurface utilities, *Adv. Eng. Inf.* 51 (2022) 101498, <https://doi.org/10.1016/j.aei.2021.101498>.
- [41] J.M. Huang, S.K. Ong, A.Y.C. Nee, Real-time finite element structural analysis in augmented reality, *Adv. Eng. Softw.* 87 (2015) 43–56, <https://doi.org/10.1016/j.advengsoft.2015.04.014>.
- [42] Y. Turkan, R. Radkowski, A. Karabulut-Ilgu, A.H. Behzadan, A. Chen, Mobile augmented reality for teaching structural analysis, *Adv. Eng. Inform.* 34 (2017) 90–100, <https://doi.org/10.1016/j.aei.2017.09.005>.
- [43] J. Huang, S.K. Ong, A.-Y.-C. Nee, An approach for augmented learning of finite element analysis, *Comput. Appl. Eng. Educ.* 27 (2019) 921–933, <https://doi.org/10.1002/cae.22125>.
- [44] J.M. Huang, S.K. Ong, A.Y.C. Nee, *An Augmented Reality Platform for Interactive Finite Element Analysis*. Springer Handbook of Augmented Reality, Springer International Publishing, Cham, 2023, pp. 533–574.
- [45] J. Xu, Z. Zhou, Visualization of Finite Element Analysis Deformation Results Based on HoloLens, *Xitong Fangzhen Xuebao/j. Syst. Simul.* 33 (2021) 109–117. <https://doi.org/10.16182/j.issn1004731x.joss.19-0201>.
- [46] E. Poh, K. Liong, J.S.A. Lee, Mixed Reality Interface for Load Application in Finite Element Analysis, *Lect. Notes Comput. Sci. (incl. Subser. Lect. Notes Artif. Intell. Lect. Notes Bioinform.)* 12774 (2021) 470–483, https://doi.org/10.1007/978-3-030-77626-8_32.
- [47] C.P. Cheng Jack, K. Chen, W. Chen, State-of-the-Art Review on Mixed Reality Applications in the AECO Industry, *J. Constr. Eng. Manag.* 146 (2020) 0319009, [https://doi.org/10.1061/\(ASCE\)CO.1943-7862.0001749](https://doi.org/10.1061/(ASCE)CO.1943-7862.0001749).
- [48] A. Logg, C. Lundholm, M. Nordaas, Solving Poisson's Equation on the Microsoft HoloLens, in: *Proceedings of the Vrst'17: 23rd Acm Symposium on Virtual Reality Software and Technology*, Gothenburg, Sweden, 8–10 November 2017.
- [49] Fang Xu, et al., Improving indoor wayfinding with AR-enabled egocentric cues: a comparative study, *Adv. Eng. Informatics* 59 (2024) 102265. <https://doi.org/10.1016/j.aei.2023.102265>.
- [50] A. Logg, C. Lundholm, M. Nordaas, Finite element simulation of physical systems in augmented reality, *Adv. Eng. Softw.* 149 (2020) 102902, <https://doi.org/10.1016/j.advengsoft.2020.102902>.
- [51] K. Malek, F. Moreu, Realtime conversion of cracks from pixel to engineering scale using Augmented Reality, *Autom. Constr.* 143 (2022) 104542, <https://doi.org/10.1016/j.autcon.2022.104542>.
- [52] K. Malek, A. Mohammadkhorasani, F. Moreu, Methodology to integrate augmented reality and pattern recognition for crack detection, *Comput. Aided Civ. Inf. Eng.* 38 (8) (2023) 1000–1019, <https://doi.org/10.1111/micc.12932>.
- [53] Al-Sabbag, Zaid Abbas, Chul Min Yeum, Sriram Narasimhan, Interactive defect quantification through extended reality, *Advanced Engineering Informatics* 51 (2022) 101473. <https://doi.org/10.1016/j.aei.2021.101473>.
- [54] Zhong Wang, et al., User-centric immersive virtual reality development framework for data visualization and decision-making in infrastructure remote inspections, *Adv. Eng. Informatics* 57 (2023) 102078. <https://doi.org/10.1016/j.aei.2023.102078>.
- [55] Philipp A. Rauschnabel, et al., What is XR? Towards a framework for augmented and virtual reality, *Computers in human behavior* 133 (2022) 107289. <https://doi.org/10.1016/j.chb.2022.107289>.
- [56] J. Koo, S. Yoon, Simultaneous in-situ calibration for physical and virtual sensors towards digital twin-enabled building operations, *Adv. Eng. Inf.* 59 (2024) 102239, <https://doi.org/10.1016/j.aei.2023.102239>.
- [57] Ting-Hao Li, et al., Efficient evaluation of misalignment between real and virtual objects for HMD-Based AR assembly assistance system, *Advanced Engineering Informatics* 59 (2024) 102264. <https://doi.org/10.1016/j.aei.2023.102264>.
- [58] D. Kido, T. Fukuda, N. Yabuki, Assessing future landscapes using enhanced mixed reality with semantic segmentation by deep learning, *Adv. Eng. Inf.* 48 (2021) 101281, <https://doi.org/10.1016/j.aei.2021.101281>.
- [59] M. Agüero, et al., Visualization of real-time displacement time history superimposed with dynamic experiments using wireless smart sensors and augmented reality, *Earthq. Eng. Vib.* (2023) 1–16, <https://doi.org/10.1007/s11803-023-2184-x>.
- [60] E. Wyckoff, M. Ball, F. Moreu, Reducing gaze distraction for real-time vibration monitoring using augmented reality, *Struct. Control Health Monit.* 29 (10) (2022) e3013.

- [61] Z.A. Al-Sabbag, C.M. Yeum, S. Narasimhan, Enabling human-machine collaboration in infrastructure inspections through mixed reality, *Adv. Eng. Inf.* 53 (2022) 101709, <https://doi.org/10.1016/j.aei.2022.101709>.
- [62] S.Z. Wu, L. Hou, G.M. Zhang, H.S. Chen, Real-time mixed reality-based visual warning for construction workforce safety, *Autom. Constr.* 139 (2022), <https://doi.org/10.1016/j.autcon.2022.104252>.
- [63] O.R. Ogunsejju, et al., Mixed reality environment for learning sensing technology applications in Construction: A usability study, *Adv. Eng. Inf.* 53 (2022) 101637, <https://doi.org/10.1016/j.aei.2022.101637>.
- [64] Spatial anchors. Available online: <https://learn.microsoft.com/en-us/windows/mixed-reality/design/spatial-anchors> (accessed on 1 Sep 2023).
- [65] Scene understanding. Available online: <https://learn.microsoft.com/en-us/windows/mixed-reality/design/scene-understanding> (accessed on 1 Sep 2023).
- [66] K. El Ammari, A. Hammad, Remote interactive collaboration in facilities management using BIM-based mixed reality, *Autom. Constr.* 107 (2019), <https://doi.org/10.1016/j.autcon.2019.102940>.
- [67] H.S. Kim, S.K. Kim, A. Borrmann, L.S. Kang, Improvement of realism of 4D objects using augmented reality objects and actual images of a construction site, *KSCE J. Civ. Eng.* 22 (2018) 2735–2746, <https://doi.org/10.1007/s12205-017-0734-3>.
- [68] A. Prabhakaran, A.M. Mahamadu, L. Mahdjoubi, Understanding the challenges of immersive technology use in the architecture and construction industry: a systematic review, *Autom. Constr.* 137 (2022), <https://doi.org/10.1016/j.autcon.2022.104228>.
- [69] J. Chalhoub, S.K. Ayer, Using Mixed Reality for electrical construction design communication, *Autom. Constr.* 86 (2018) 1–10, <https://doi.org/10.1016/j.autcon.2017.10.028>.
- [70] N. Ham, S.-H. Lee, Empirical study on structural safety diagnosis of large-scale civil infrastructure using laser scanning and BIM, *Sustainability* 10 (11) (2018) 4024, <https://doi.org/10.3390/su10114024>.
- [71] F. Bosche, B. Biotteau, Terrestrial laser scanning and continuous wavelet transform for controlling surface flatness in construction - a first investigation, *Adv. Eng. Inform.* 29 (3) (2015) 591–601, <https://doi.org/10.1016/j.aei.2015.05.002>.
- [72] Q. Wang, M.-K. Kim, Applications of 3D point cloud data in the construction industry: A fifteen-year review from 2004 to 2018, *Adv. Eng. Inform.* 39 (2019) 306–319, <https://doi.org/10.1016/j.aei.2019.02.007>.
- [73] H. Yang, X. Xu, I. Neumann, Laser Scanning-Based Updating of a Finite-Element Model for Structural Health Monitoring, *IEEE Sensors J.* 16 (7) (2016) 2100–2104, <https://doi.org/10.1109/JSEN.2015.2508965>.
- [74] “3D point cloud and mesh processing software Open Source Project.” <https://www.cloudcompare.org/> (accessed on 30 March 2023).
- [75] J. Bedkowski, K. Majek, P. Musialik, A. Adamek, D. Andrzejewski, D. Czekaj, Towards terrestrial 3D data registration improved by parallel programming and evaluated with geodetic precision, *Autom. Constr.* 47 (2014) 78–91, <https://doi.org/10.1016/j.autcon.2014.07.013>.
- [76] B. Conde-Carnero, B. Riveiro, P. Arias, J.C. Caamano, Exploitation of geometric data provided by laser scanning to create FEM structural models of bridges, *J. Perform. Constructed Facilities* 30 (3) (2016) 04015053, [https://doi.org/10.1061/\(ASCE\)CF.1943-5509.0000807](https://doi.org/10.1061/(ASCE)CF.1943-5509.0000807).
- [77] Performance — MRTK2. Available online: <https://learn.microsoft.com/en-us/windows/mixed-reality/mrtk-unity/mrtk2/performance/perf-getting-started?view=mrtkunity-2022-05> (accessed on 29 January 2024).